LAPPEENRANTA UNIVERSITY OF TECHNOLOGY
LUT School of Energy Systems
LUT Mechanical Engineering

Changyang Li

DESIGN AND ANALYSIS OF ROBOT FOR THE MAINTENANCE OF DIVERTOR IN DEMO FUSION REACTOR

Examiner(s): Adjunct professor Huapeng Wu
Professor Harri Eskelinen

ABSTRACT

Lappeenranta University of Technology
LUT School of Energy Systems
LUT Mechanical Engineering

Changyang Li

Design and analysis of robot for the maintenance of divertor in DEMO fusion reactor

Master's thesis

2017

76 pages, 69 figures, 12 table

Examiners: Adjunct professor Huapeng Wu
Professor Harri Eskelinen

Keywords: DEMO, remote handling, end-effector, divertor, fusion

This thesis aims to design divertor cassette remote handling end-effector, then comparison between these concepts and other existed concepts are carried out. The concepts are modelled and analyzed by using modeling software and finite element analysis software.

In mechanical design phase, main components in each concept are selected or designed, such as bearings and rails. The mechanism of the concepts is introduced also. Two concepts are cantilever structures, however, the third concept is simple supported beam structure, which provides more stiffness. Furthermore, two cantilever structures adopt 4-UPU parallel manipulator to eliminate the clearance between the inner and outer blankets, while another concept simply uses hydraulic jacks to achieve this goal. In analysis phase, finite element method is used to test the structure until the calculated results satisfy the requirements. Equivalent stress and total deformation are calculated to compare different concepts stability.

Finally, the advantages of each concepts are analyzed as well as the future improvements of each concepts are pointed out.

ACKNOWLEDGEMENTS

This master thesis was carried out during 2017 in Laboratory of Intelligent Machines, Lappeenranta University of Technology, Finland.

I owe my deepest gratitude to my supervisor professor Huapeng Wu who provide financial support, shows patience and provides valuable suggestions. And I express my gratitude to my professor Harri Eskelinen who provide me this priceless platform to apply my knowledge. And I would also give my sincere pleasure to my friends who give me many remarkable moments and encouragement during my daily life in Lappeenranta: Mr. Xin Wang, Ms. Bingyan Mao, Ms. Xinxin Yu, Dr. Shanshuang Shi, Dr. Ming Li, Mr. Tao Zhang, Ms. Xiaoyi Chen, Ms. Joanne Song, Ms. Qifeng Hao, Mr. Xin Mei.

Last but not least, deeply love and thanks goes to my parents and friends, they give me freedom to choose what I like and motivation during my daily life and studying in Finland!

Changyang Li
Lappeenranta 23.11.2017

TABLE OF CONTENTS

TABLE OF FIGURES

TABLE OF TABLES

LIST OF SYMBOLS AND ABBREVIATIONS

F_a	Axial load applied on bearing [N]
F_{ac}	Theoretically calculated axial load [N]
f_L	Load factor based on application
F_r	Radial load applied on bearing [N]
F_{rc}	Theoretically calculated radial load [N]
f_w	Load factor based on force calculation

CCs	Correction Coils
CFETR	China Fusion Engineering Test Reactor
CMM	Cassette Multifunctional Mover
CS	Central Solenoid
CTM	Cassette Toroidal Mover
D	Deuterium
DEMO	DEMOnstration Power Station
DOF	Degree of Freedom
EURATOM	European Atomic Energy Community
FEM	Finite Element Method
ITER	International Thermonuclear Experimental Reactor
JET	Joint European Tours
KSTAR	Korea Superconducting Tokamak Advanced Research
LM	Linear Motion
PF	Poloidal Field
RH	Remote Handling
T	Tritium
TF	Toroidal Field
UP	Ultra-Super Precision
VTT	Finnish National Technology Research Center
VV	Vacuum Vessel

1 INTRODUCTION

Remote handling gives the feasibility to operator to do manual handling work in special work site, while the manipulator itself is located in an environment that will cause damage to human body, such as high temperature and radiation site (ITER, 2017).

1.1 ITER introduction

ITER means “the way” in Latin and full name is International Thermonuclear Experimental Reactor. ITER is an international research and engineering megaproject. Its aims are to demonstrate fusion energy can be sued in peaceful way. It will be the first fusion device to produce net energy and it will keep the operation of fusion for certain time. ITER was first launched in 1985. The ITER members include China, the European Union, India, Japan, Korea, Russia and the United States. There are different tokamak machines in each countries, for example, JT-60SA in Japan (Di Pietro et al., 2014), KSTAR (Korea Superconducting Tokamak Advanced Research) in Korea (Bak et al., 2006), ST40 from UK (Gryaznevich and Asunta, 2017), EAST in China and so on. In the following section, some tokamak examples are listed.

The tokamak chamber of ITER has radius of 2 meters, the core temperature is 100 million degrees and power density are 500000 W/m^3, where in sun, it has 0.7 million kilometers as radius, 10 million degrees as core temperature and only 0.01 W/m^3 as power density. The ITER will be 29 m in high, 28 m in diameter and weight 23000 tones once being built. ITER field is around 10 tesla and super conducting magnet energy is around 51 GJ. (ITER, 2017, Aymar, 1997, Holtkamp, 2007.)

Fusion is the operation where two hydrogen isotopes D (deuterium) and T (tritium) are reacted, these light hydrogen atoms can produce a heavier element, helium and one neutron. The mass of the helium atom is not the sum amount of those light hydrogen atoms because mass lost, and huge amounts of energy are generated. The most efficient fusion reaction at the moment is achieved by D and T fusion, which can produce the highest energy at “lowest” temperatures compared with other sets. A simple illustration of fusion reaction can be seen in Figure 1. (ITER, 2017.)

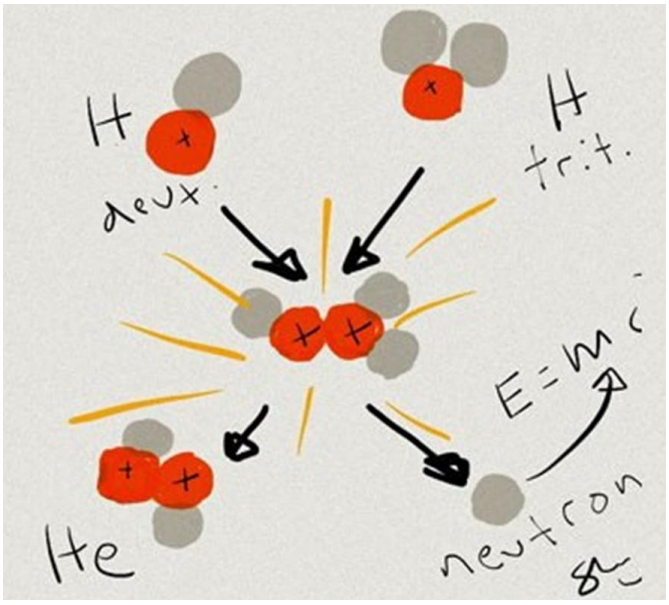

Figure 1. Atoms reaction in fusion reaction (ITER, 2017).

1.2 DEMO introduction

DEMO's full name is DEMOnstration Power Station, it is a nuclear fusion power station and it is proposed to be built after ITER experimental nuclear fusion reactor. A route of fusion power development can be seen in Figure 2 (McAdams, 2014). The final design of DEMO is based on the results obtained from ITER and other fusion experiments. The aim of DEMO is to demonstrate that fusion can be used to produce electricity in commercial usage. (Thomas et al., 2013.) The main differences between ITER and DEMO can be seen in Table 1 (Federici et al., 2014).

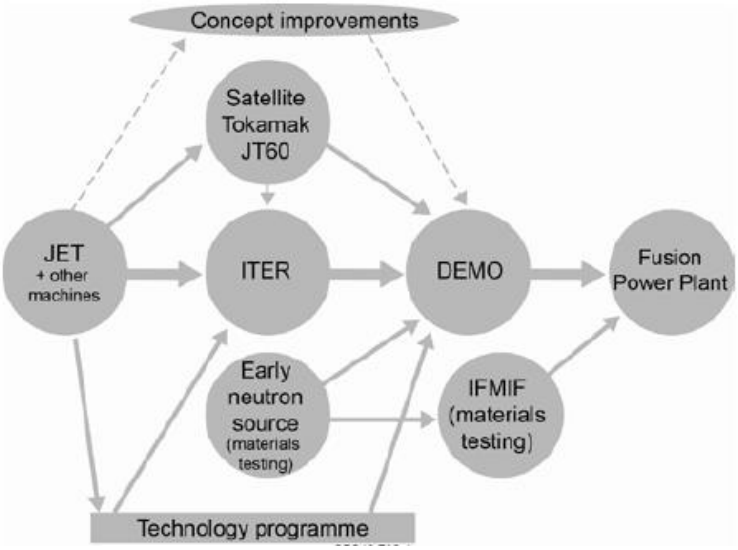

Figure 2. The route to fusion power (McAdams, 2014).

Table 1. Main differences between ITER and DEMO (Federici et al., 2014).

ITER	DEMO
Experimental device with physics and technology development missions	Nearer to a commercial power plant but with some development missions
400 s pulses, long dwell time	Long pulses (>2 h) or steady state
Experimental campaigns. Outages for maintenance, component replacements	Maximize availability
Large number of diagnostics	Only diagnostics required for operation
Multiple H&CD systems	Optimized set of H&CD systems
Large design margins, necessitated by uncertainties and lack of fully appropriate design codes	With ITER (and other) experience, design should have smaller uncertainties
Cooling system optimized for minimum stresses and sized for modest heat rejection	Cooling system optimized for electricity generation efficiency (e.g. much higher temperature)
Unique one-off design optimized for exptl. goals	Move towards design choices suitable for series production
No tritium breeding requirement (except very small quantity in TBMs)	Tritium breeding needed to achieve self-sufficiency
Conventional 316 stainless steel structure for in-vessel components	Nuclear hardened, novel reduced activation materials as structure for breeding blanket
Very modest lifetime n-fluence, low dpa and He production	High fluence, significant in-vessel materials damage
Licensed as nuclear facility, but like a laboratory, not a reactor	Licensing as nuclear reactor more likely
Licensing as experimental facility	Stricter approach may be necessary to avoid large design margins
"Progressive start-up" permits staged approach to licensing	"Progressive start-up" should also be possible (e.g. utilize a "starter" blanket using moderate-performance materials and then switch to blankets with a more advanced-performance material after a few MW-year/m^2)
During design, licensing in any ITER party had to be possible	Fewer constraints

1.3 CFETR introduction

CFETR represents the Chinese Fusion Engineering Testing Reactor and it will be built between ITER and DEMO. There are three goals that should be achieved with CFETR, first one is to reach 50-200 MW fusion power, second goal is reach 30% to 50% duty cycle time and the third goal to achieve self-sufficient tritium breeding by the blanket. (Song et al., 2014, Zhao et al., 2015.)

1.4 EAST introduction

EAST represents the Experimental Advanced Superconducting Tokamak, which is located in China and it was approved by the Chinese government in 1989. Its goal was to study the

physics issues of the advanced steady-state tokamak operations. The EAST tokamak machine has height of 10 meters, diameter of 7.6 meters and weight of 414 tons. (Wu, 2007.) There are some progresses that EAST achieved in past few years, on 2nd of November, 2016, EAST became the 1st tokamak to sustain long-pulse H-mode plasma for over 60 seconds (English.ipp.cas.cn, 2017). On 3rd of July, 2017, EAST became the 1st tokamak to achieve a stable 101.2 seconds steady-state high confinement plasma. (EurekAlert!, 2017.)

1.5 Tokamak

Tokamak is an experimental machine, it can generate energy from fusion reaction. The energy is produced via fusion of atoms and then the walls of the vessel can absorb the energy in the form of heat. The heat is further heat the water in the pipe to produce steam. In the end, electricity is generated by the way of turbines and generators, which is like other conventional power plant. (ITER, 2017.)

There are mainly five components in the Tokamak, which are magnets, VV (vacuum vessel), blanket, divertor and cryostat.

The ITER experiments will be happened inside the VV, which is a sealed steel container, it acts as the first safety containment barrier and it needs to support electromagnetic loads during the whole operation (ITER, 2017). Moreover, it needs to withstand any unpredicted accidents without losing its confinement. The plasma particles move around the magnetic field continuously without touching the walls. (Ioki, 1995, Mozzillo et al., 2016.) Magnet system consists of numbers of superconducting coils include 18 TF (toroidal field) coils, 1 CS (central solenoid), 6 PF (poloidal field) coils and 18 CCs (correction coils). The location of magnets coils can be seen in Figure 3. (Mitchell et al., 2008, Mitchell et al., 2009.) The blanket component is a physical boundary that can isolate plasma and heat, it has interfaces with some key components, such as VV and in-vessel coils (Mozzillo et al., 2016). About the cryostat, it create vacuum environment to insulate the heat from magnet system and it can be seen as a container of the entire basic system of the Tokamak (Doshi et al., 2011). As for the divertor, it will be introduced separately in next section since it is the main component involved in this thesis.

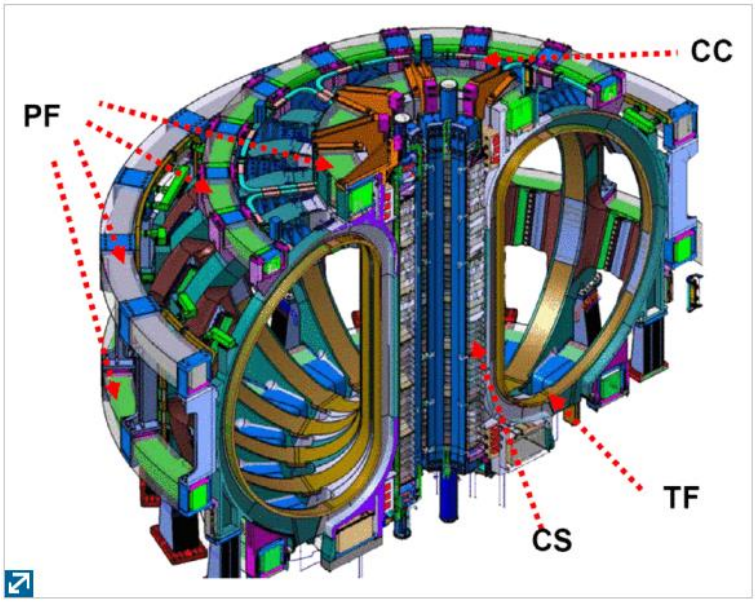

Figure 3. The ITER coils (Mitchell et al., 2008).

1.6 Divertor

Divertor is situated at the bottom of the VV. When fusion reaction starts, it will generate heat and ash, which need to be extracted and these are the first function of divertor, second function is to minimize plasma contamination and third function is to protects the surrounding walls in the environment where thermal and neurotic loads are existed. A divertor from ITER can be seen in Figure 4. In ITER, divertor is consist of 54 cassettes, each cassette is supported by stainless steel structure and it also has three plasma-facing components, which are inner vertical target, outer vertical target and the dome. Each cassette weights 9 tones and maximum total thermal load is 204 MW. (ITER, 2017.) Due to erosion of divertor, the divertor is expected to be replaced every 2-2.5 full-power year (Maisonnier, 2008).

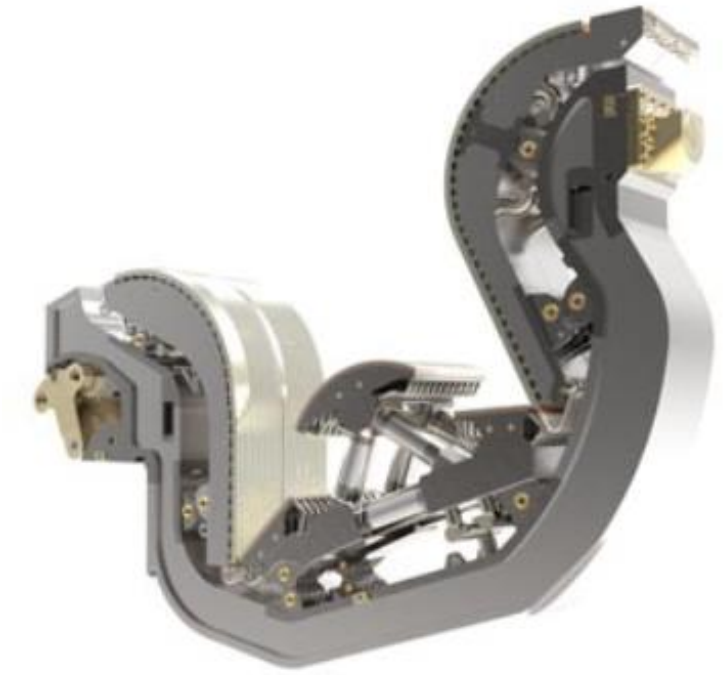

Figure 4. Divertor cassette of ITER (ITER, 2017).

The divertor can be seen as consumable components because during the divertor operation, erosion can happens on the divertor plates. There are many aspects that may affect the erosion, for example, chemical sputtering, slow transients and disruption erosion. Moreover, most of the alpha particle power and the He ash must be exhausted from divertor to keep the erosion rates in acceptable level. As a result, the divertor needs to be replaced regularly to assure the smooth operation. (Tivey et al., 1999, Pacher, 1997, Janeschitz et al., 1995.)

DEMO divertor cassette can be seen in Figure 5. The size of DEMO divertor cassette has significant reduction compared with that of ITER divertor cassette. It is equipped with dual coolant circuit system and these two piping systems can run individually through the plasma facing components and the cassette body. Out board and inboard baffle parts are no longer attached to cassette and breeding blanket. So that the tritium breeding ratio increases from 1.13 to 1.19 contributed from additional breeding areas. (You et al., 2016, Carfora et al., 2015.) The first version of divertor was developed in 2014, there were 16 ports for the maintenance of divertor and three cassettes could be operated from each port. In the revised cassette design model in 2015, the cassettes amounts are estimated to be 54. (You et al., 2016.)

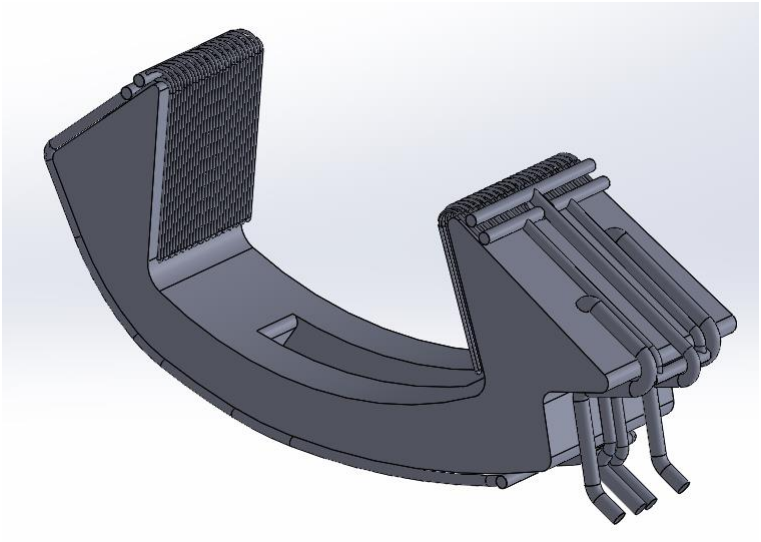

Figure 5. Divertor cassette of DEMO.

1.7 Remote handling

RH (Remote handling) has crucial role in ITER tokamak. It is impossible to do any change or repair during the nuclear operation due to the extreme atmosphere. Heavy heat load and thermal stress generated during the operation may cause damage to components themselves. (Di Gironimo et al., 2015.) There are different types of damage that can occur, such as leakage of vacuum system, local diagnosis, heating system failure and replacement of divertor part. So, maintenance is needed, however, it is impossible to be carried out by human due to the extreme circumstance. Here list some requirements of divertor RH system:

- Reliability: RH system in vessel should be able to work in an environment where the radiation intensity is lower than 500 Gy/h.
- Capacity: RH system should have great load capacity and safety margin of 10 t, which is the weight of cassette.
- Material: high strength and radiation resistant material should be used.
- Efficiency: The whole divertor system replacement time should satisfy the duty time.
- Working environment: the RH system should be able to operate between 20°C and 50°C, and in dust environment where involves tritium and other activated dust. (Song et al., 2014)

RH is needed in many cases, such as blanket and divertor RH. In this thesis, RH is focus on the transportation of cassette in DEMO, a RH system is designed in each port and 3 cassettes can be transported to specified location in sequence from this port. The overall circuit can

be seen in Figure 6, firstly, the cassette is transported to vessel area, which is in center cassette position, and then the cassette is transported toroidal to left or right side, cassette in another side is transported in the same manner, in the end, the third cassette is transported directly to center cassette position. (Videnoja et al., 2017.)

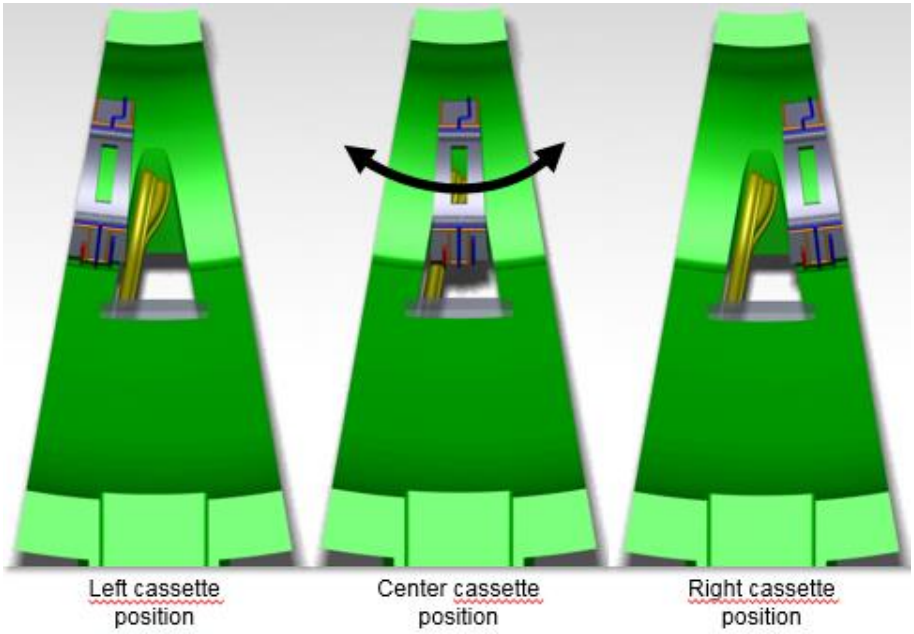

Figure 6. Toroidal transportation of the cassette (Videnoja et al., 2017).

Here list few RH examples in previous or present projects.

1.7.1 JET RH

JET represents the Joint European Torus project, which was built by EURATOM (European Atomic Energy Community) in 1970's to check the feasibility of nuclear fusion controlling. RH system was designed to allow maintenance in tokamak. The movement of RH system in tokamak is based on the skilled technician's movement even when the work area has high radiation levels. The RH system is based on deployment of a two arms, force reflecting, Maser-Slave, servo-manipulator system and vision system, which allow operator to see the performance of the work. A scene of technician working can be seen in Figure 7. Each arm has 7 DOFs (Degree of freedoms) and the lift capacity is 20 kg, the sensitivity of the force reflection is 100 gm. (Rolfe, 1999.)

Figure 7. JET RH approach (Rolfe, 1999).

The manipulator is positioned by using 10 m long articulated boom, which can be seen in Figure 8. The whole structure has 19 DOFs and it works like robot, which can be controlled by joystick or keyboard. (Rolfe, 1999.)

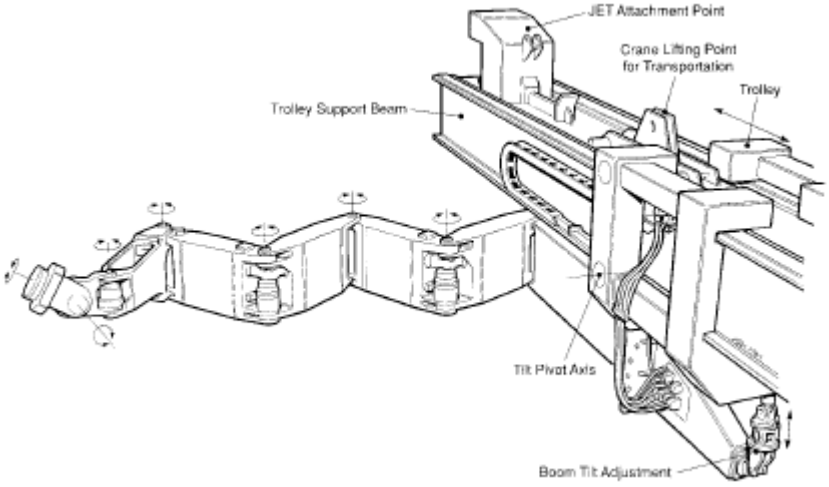

Figure 8. JET articulated boom (Rolfe, 1999).

1.7.2 ITER RH

RH system is crucial part in ITER assembly. There are mainly two phases assembly, the first phase includes assembly of the cryostat, magnets, VV, ports, in-vessel coils, heating systems and diagnostic systems. In the second stage, PFC (Plasma-Facing Components), blanket and divertor systems will be assembled. (Macklin et al., 2015.)

In ITER RH, each cassette is around 9 tones and its external dimensions are 3.5 m*2.1 m*0.8 m in length, height and width separately. There are some prototypes in the RH system. For example, VTT (The Finnish National Technology Research Center) and Tampere University of Technology, Finland together has built prototype CMM (cassette multifunctional mover) and CTM (cassette toroidal mover) in Divertor Remote Maintenance Test Platform. There are two types of devices integrated in this RH system, which are CMM and CTM, the prototype CMM and CTM can be seen in Figure 9. (Maisonnier, Martin and Palmer, 2001. Di Gironimo et al., 2013.) Firstly, the cassette will be transported to location by mover in horizontal direction and then transported in toroidal direction to location by water hydraulic cylinder since it has high force capacity. And CMM can work in the atmosphere of 1 MGy total gamma radiation dose at a maximum 100 Gy/h dose rates. (Palmer et al., 2005.)

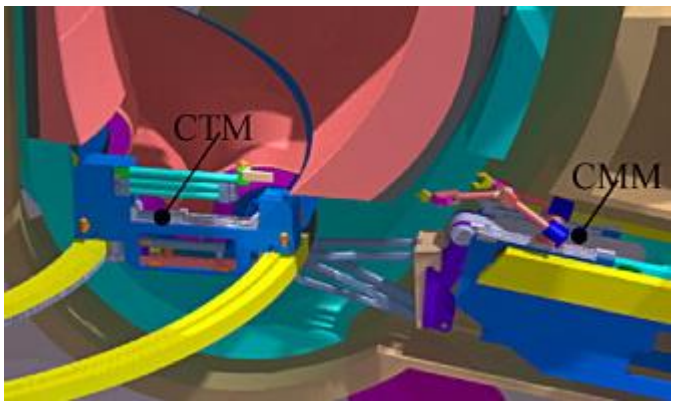

Figure 9. Prototype CMM and CTM (Song et al., 2014).

1.7.3 DEMO RH

Blanket segments and divertor cassettes require periodic replacement in DEMO fusion reactor. When the DEMO fusion reactor is shutdown, the dose rate in the environment should be controlled as low as possible during the RH operation and the shutdown dose analyses were carried out by using two different codes, which are MCNP-5 (X-5 Monte Carlo Team, 2005) and DCHAIN-SP2001 (T. Kai, et al., 2001). The estimated dose rate is 0.01 Gy/h in the maintenance ports when pipe cutting and welding are in operation. The estimated dose rate is 0.1 Gy/h in divertor cassette, the reason why the estimated dose rate in maintenance ports is smaller than that in divertor cassette is photos are absorbed by the in VV components once they are arisen. (Someya et al., 2017)

1.7.4 CFETR RH

CFETR represents China Fusion Engineering Test Reactor, its main parameters compared with ITER is illustrated in Table 2.

Table 2. Parameters of CFETR and ITER (Song et al., 2014).

Parameter	CFETR	ITER
Plasma current I_p*(MA)*	8.5/10	15
Major radius of plasma *R (m)*	5.7	6.2
Minor radius of plasma *a (m)*	1.6	2.0
Central magnetic field *Bt (T)*	4.5/5.0	5.3
Elongation ratio κ	1.8	1.70/1.85
Triangle deformation δ	0.4	0.33/0.48
Number of TF coils *(N)*	16	18

Divertor requires few times replacement during CFETR lifetime. RH system of divertor maintenance in CFETR relies on CMM and CTM. There are four lower divertor handling ports and cassettes are transported by the CMM firstly, followed by CTM in toroidal rail. The structure of CFETR RH can be seen in **Figure 10**. (Song et al., 2014.)

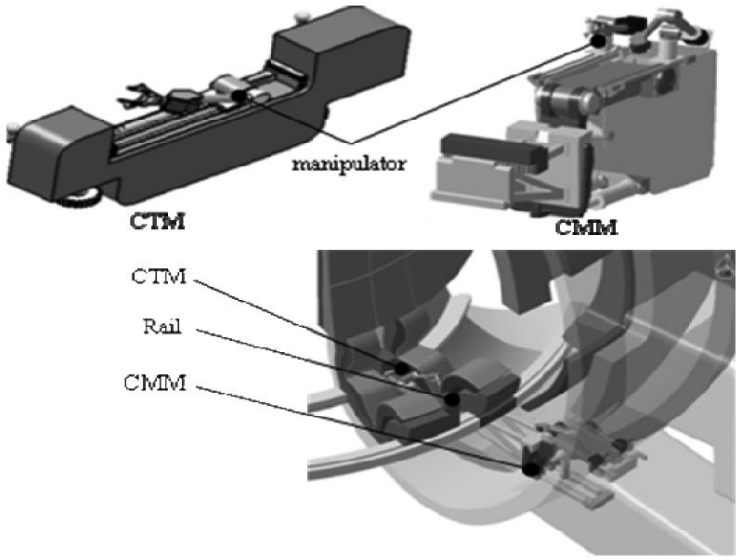

Figure 10. CFETR RH system (Song et al., 2014).

1.8 Aim of the thesis

The aim of this thesis is divertor cassette end-effector of DEMO fusion reactor development and respective performance evaluation. The research problem is lacking of divertor cassette end-effector concepts. There are some existed concepts from VTT, but there should be more concepts so that all the concepts can be compared and the best concepts can be selected

among all the concepts. The research question is why these innovative concepts are better or what the improvements are when these concepts are compared to the existed concepts. There are many design methodologies, in this case, it is iterative process involving modeling, analysis. The benefit of this methodology is that it can develop the previous model and lead to better design. (Nielsen, 1993.) The end-effector should be able to transport the cassette to desired location and it should be able to make minor position change to eliminate the clearance. There are three existed cassette end-effector concepts proposed by VTT, these three concepts are concept #1, #2 and #3, which will be introduced in following sections. The cassette end-effector concepts include description of innovative cassette end-effector concepts, kinematic simulation on the mechanism principles of the developed concepts, preliminary static analysis and flexibility investigation. Firstly, concepts of cassette end-effector will be carried out, then the geometry of structure will be optimized by satisfying the desired equivalent stress and total deformation, which are calculated by using ANSYS Workbench 16.0 software. Kinematic simulation is achieved by using SOLIDWORKS 2017 software animation function and robot movements are analyzed by using mathematic method also.

2 EXISTED CONCEPTS

In this chapter, 3 existed concepts are introduced. All concepts involve transportation of the cassette between cask and vessel area, toroidal transportation of the cassette and vertical lifting of the cassette so that the cassette can be transported to specified location.

2.1 Transportation of the cassette between cask and vessel area

Firstly, the cassette is transported between cask and vessel area by mover integrated with rack and pinion. The material of mover is 42CrMo4 (R_p=900 MPa), cassette mover weight is 7 tones, there is one actuator on each side of the mover and safety factor is 5.

The suggested pinion parameters are:

- pinion width: 160 mm
- pinions diameter: 180 mm
- module: 10
- number of teeth: 18
- pressure angle: 20°
- σ_{max}=711 MPa (σ/R_p=1.2)

The model of rack and pinion can be seen in Figure 11. (Videnoja et al., 2017.)

Figure 11. Rack and pinion (Videnoja et al., 2017).

As for the mover supporting wheels, the material is the same as rack and pinion, which is 42CrMo4 (R_p=900 MPa), 4 wheels layout and safety factor is 5.

The suggested wheels parameters are: wheels width is 120 mm and wheels diameter is 360 mm. (Videnoja et al., 2017.)

2.2 Toroidal transportation of the cassette

All the concepts have the same sequence of toroidal transportation, which is illustrated in Figure 6.

2.3 Vertical lifting of the cassette

Vertical lifting of cassette is needed to eliminate the clearance, single acting, spring return cylinder is used in this case.

2.4 Concept #1

Concepts #1 is toroidal transportation and lifting of the divertor cassettes. The toroidal cassette manipulator has 6 DOFs and it is located under the cassette. And 6 joints can be seen in Figure 12. Figure 12 is prismatic joints and others are revolute joints. The whole structure is cantilever structure. (Videnoja et al., 2017.)

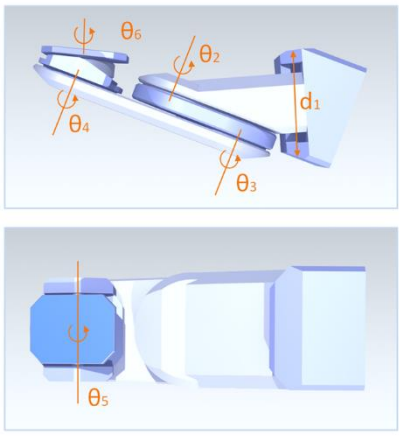

Joint	Type
d_1	Prismatic
θ_2	Revolute
θ_3	Revolute
θ_4	Revolute
θ_5	Revolute
θ_6	Revolute

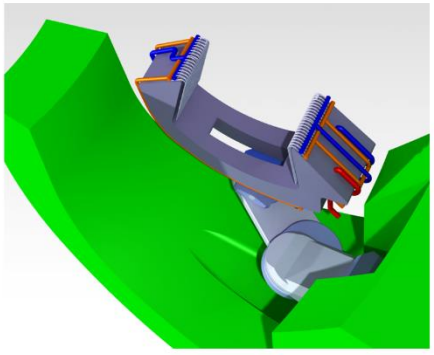

Figure 12. The overview of concept #1 (Videnoja et al., 2017).

The FEM (finite element method) results from ANSYS can be seen in Figure 13 and Figure 14. Maximum stress is approximately 40 MPa and maximum displacement is approximately 1.5 mm.

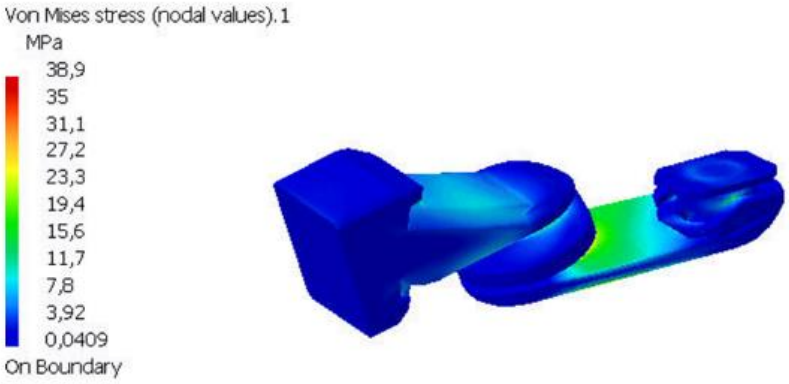

Figure 13. Concept #1 von mises stress (Videnoja et al., 2017).

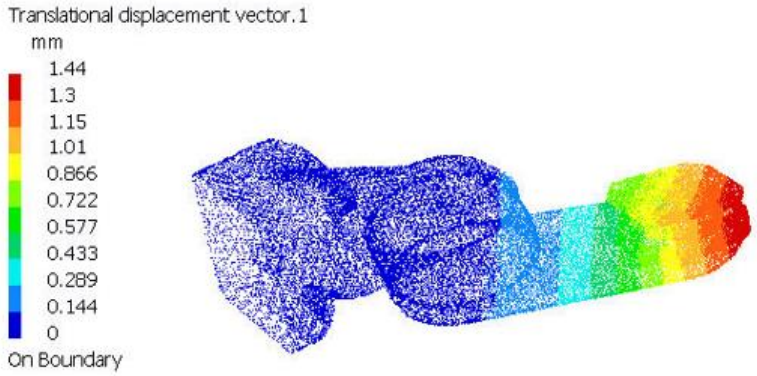

Figure 14. Concept #1 displacement (Videnoja et al., 2017).

Future work of concept #1 will be divided into three parts. First part is toroidal cassette manipulator, which includes manipulator kinematics, modelling and dimensioning of link joints, selection of sensors and FEM analysis of the updated structure. Second part is cassette interface, passive or active gripping mechanism should be designed. Third part is mover interface and end-effector change system. (Videnoja et al., 2017.)

2.5 Concept #2

Concept #2 is toroidal platform with integrated rails as shown in Figure 15. There is some space on the VV, then when the platform moves, some rails can be extended out and integrated with the rail on the platform to form two long rails, which allows toroidal movement for cassette. Then the cassette can be transported to left and right sides. (Videnoja et al., 2017.)

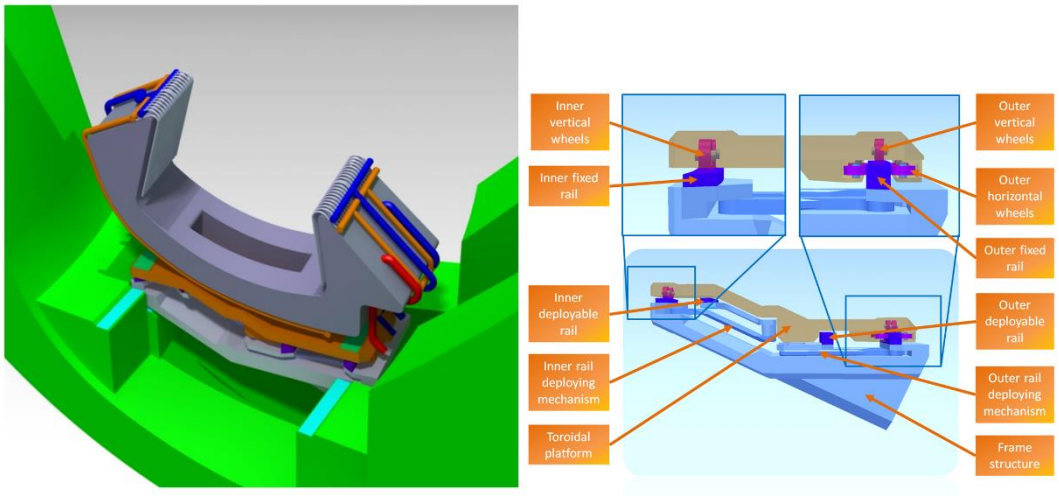

Figure 15. Overview of concept #2 (Videnoja et al., 2017).

The installation sequences of left side cassettes can be seen in Figure 16. (Videnoja et al., 2017.)

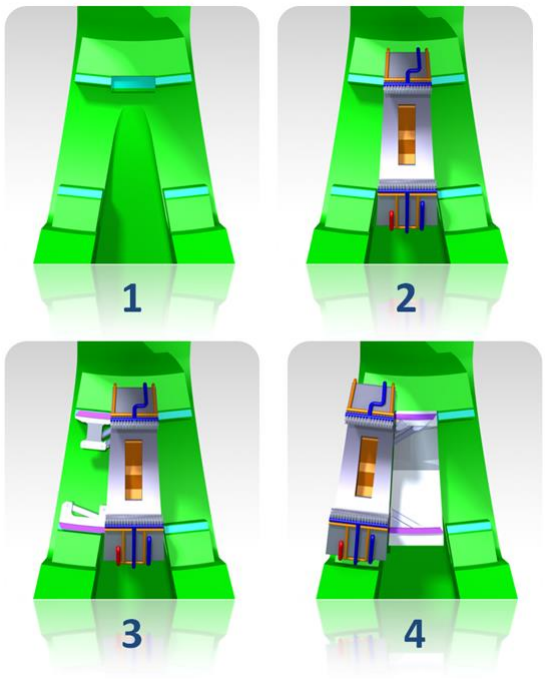

Figure 16. Installation sequence for left cassette (Videnoja et al., 2017).

Wheels are used in this structure to allow plate moves on the toroidal rail. Wheel's dimension is calculated based on wheel surface pressure on rails and shaft and bearing sizing. Outer diameter of wheel is 110 mm. And FEM results for frame structure from ANSYS can be

seen in Figure 17 and Figure 18. The maximum stress is approximately 15 MPa and maximum displacement is approximately 0.6 mm. (Videnoja et al., 2017.)

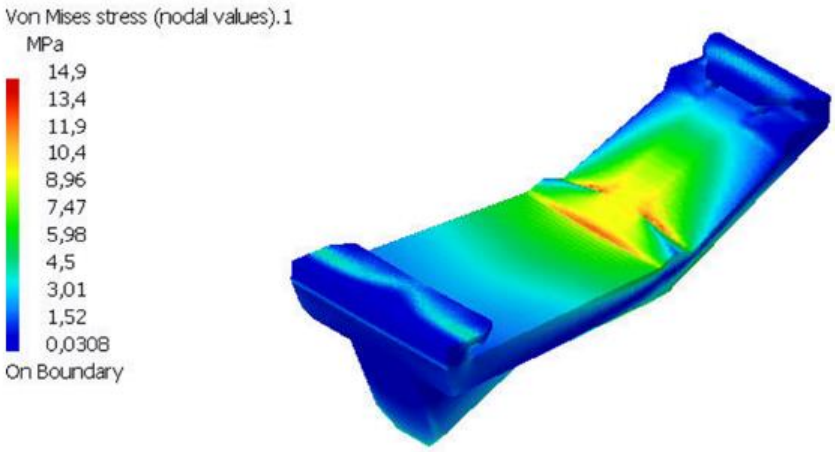

Figure 17. Concept #2 von mises stress (Videnoja et al., 2017).

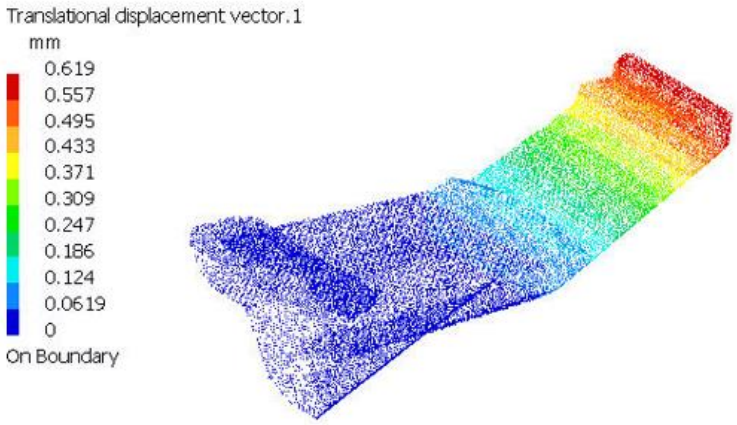

Figure 18. Concept #2 translational displacement (Videnoja et al., 2017).

Future work of concept #2 can be divided into three parts. First part is to study how to optimize the concept so that the space can be effectively used. Second part is dimensioning and modelling of actuator and rails. Third part is to design the interfaces to the vessel, cassette and mover. (Videnoja et al., 2017.)

2.6 Concept #3

Concept #3 is toroidal platform with hydraulic jacks as shown in Figure 19. There will be groves on the VV, when in operation, the structure will send the rail into the VV, then the cassette can be moved along the toroidal rail, lifting and descending are achieved by

hydraulic jacks. Maximum stress is approximately 59 MPa for the hydraulic jack frame and 12 MPa for the support platform. Maximum displacements are less than 1 mm in both cases. (Videnoja et al., 2017.)

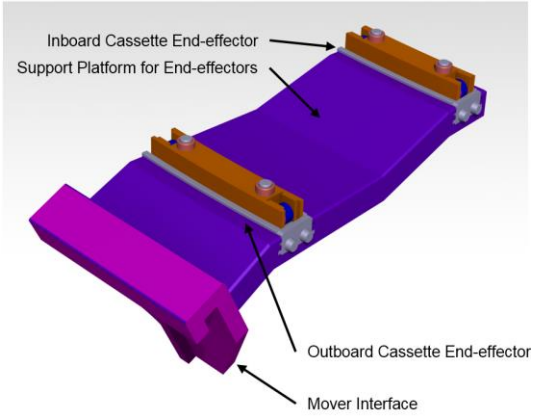

Figure 19. Overview of concept #3 structure (Videnoja et al., 2017).

Future work of concept #3 can be divided into three parts. First part is to design the hydraulic jack, which include height optimization, orientation design. Second part is interface of vessel rail. Third part is detailed FEM analysis for the updated structure. (Videnoja et al., 2017.)

3 INNOVATIONAL CONCEPTS

In this chapter, three innovative concepts are introduced, concept #4 and concept #5 both adopt 4-UPU parallel manipulator to achieve clearance elimination while concept #6 simply use hydraulic jack and spherical joint to eliminate the clearance. The description of clearance will be introduced in following section.

There are many design requirements, which are listed below:

- The end-effector should be capable of lifting one cassette of DEMO fusion reactor, whose weight is around 7 tones.
- The end-effector should have mechanics that allow minor movement of cassette, the tilt angle should be around 10° and lift height should be around 50 mm.
- The equivalent stress of end-effector should satisfy the material properties.
- The total deformation of end-effector should be as small as possible, such as 1 mm.
- The end-effector should be simple, which can be performed as the number of DOF of the structure. So, it allows maintenance and assembly.

3.1 Concept #4

Concept #4 is introduced in this section. Structure mechanism, components and ANSYS analysis are introduced. Concept #4 is VV can be seen in Figure 20.

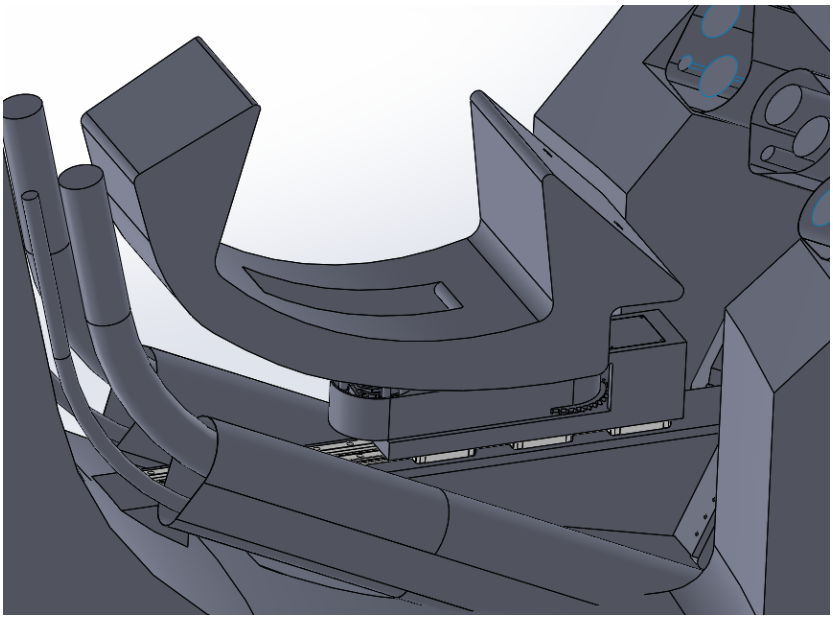

Figure 20. Concept #4 in VV.

3.1.1 Mechanism of concept #4

The overall structure can be seen in Figure 21, there are 9 main parts in this structure and they will be introduced separately. Part 1 is the rail, it supports the static load and dynamic load. Part 2 is one frame, which connects the VV and mover. Part 3 is 4-UPU parallel manipulator, the plate on the top connect the whole structure with cassette by locking system. Part 4 can be assumed as a rotating box or beam, in which 4-UPU parallel manipulator and motor are integrated inside. Part 5 is a body that connects part 4 and rail block. Part 7 is the slewing bearing that can hold heavy load during the operation. Part 8 is the rail block, here are 3 sets of blocks in parallel on the rail. Part 9 is spherical roller bearing, which allow rotation movement of part 4.

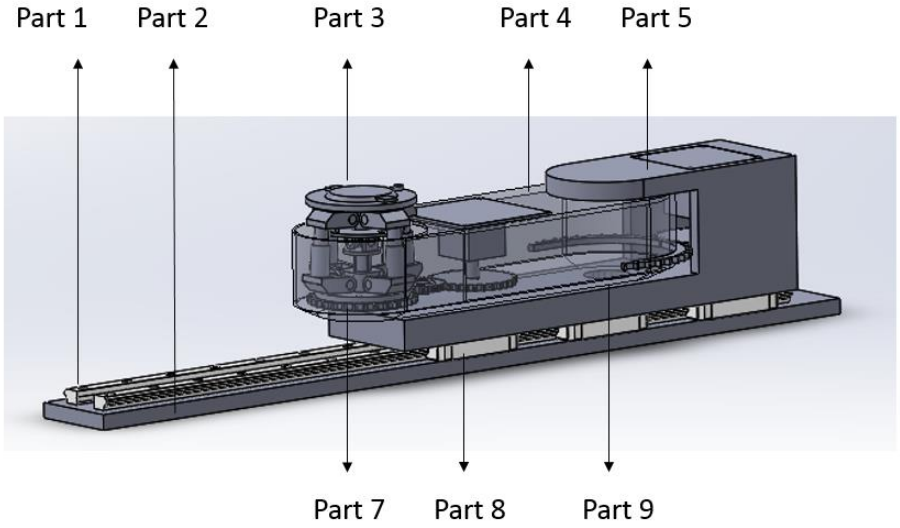

Figure 21. Concept #4 structure.

About the movement mechanism of the structure, it can be seen in Figure 22. Firstly, the whole structure will be transported to specified location by mover, here the part 2 will connect to the VV and be locked in position. Then part 5 can move along the rail, part 4 and part 3 are able to rotate, these three DOFs allow the cassette to be transported to desired location. After these operations, there is still clearance between the cassette and inner and outer blankets and it is eliminated by 4-UPU parallel manipulator, this manipulator can rotate in x and y axis and move in z axis. Details or 4-UPU parallel manipulator will be introduced in following sections.

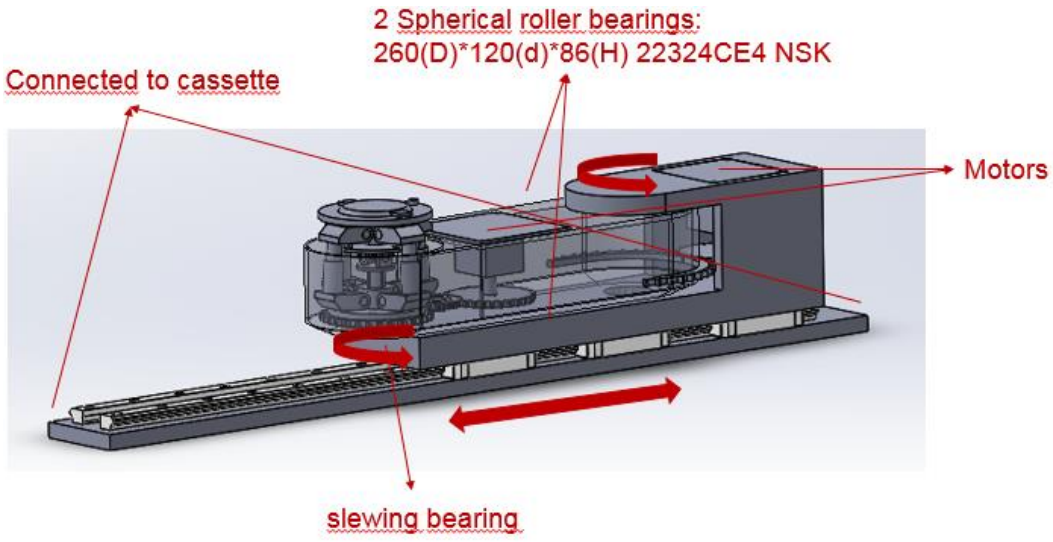

Figure 22. Overview of concept #4 mechanism.

3.1.2 Components of concept #4

In this section, main components involved in concept #4 will be introduced, the main components include mover, rail, slewing bearing, spherical roller bearings and 4-UPU parallel manipulator.

Mover

Mover can do maintenance work at each port for three cassettes. Firstly, the mover is driven and moved to specified location. Secondly, the cooling pipes and other connections are set up. Thirdly, the cassette is unlocked from VV or connected to the mover depend on the operation. In the end, mover via telescopic boom transports the cassette. In ITER, rack and pinion system is used instead, which is mentioned in previous section. (Carfora et al., 2015.) Mover is original component that can transport the cassette to desired position in the rail with an angle, in this case, the angle is 25°. It can give this concept #4 one more DOF.

Rail

The LM (linear motion) guide overview model is illustrated in Figure 23. One set of models include two rails and two blocks, balls rolls are circulated in the retainer plate. The ball contacts the raceway at 45°, so the same loads are applied in four directions, which are radial, reverse radial and lateral directions. In LM guides selection, there are wide range types of LM guides, HR type model is most used in transportation of machines. (LM Guide, 2017, p.A1-257.)

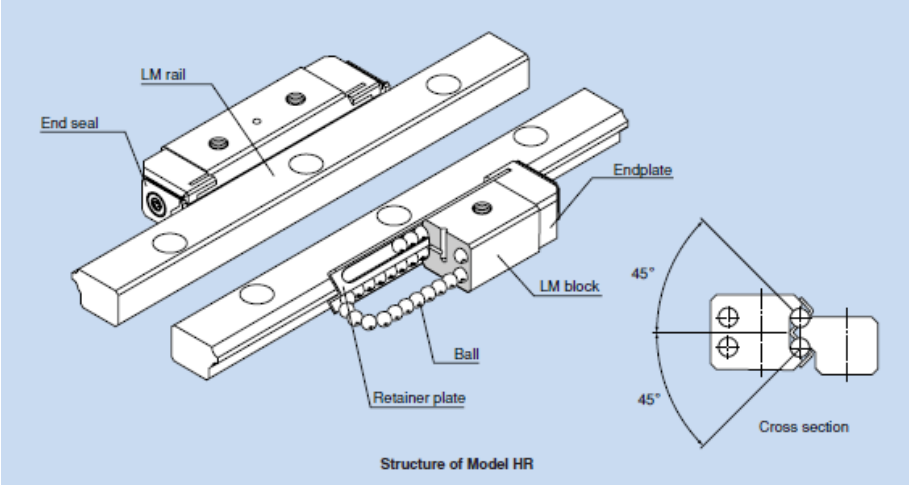

Figure 23. HR type LM guides (LM Guide, 2017, p.A1-256).

To get the dimension of the rail guide, forces and moments applied on each block should be calculated. Many companies have software for the rail guide selection, below are some figures shown the selection procedures. Two rails and three blocks in one rail set is chosen, which can be seen in Figure 24, location of each component and drive can be seen in Figure 24. Rail span is 300 mm, block span is 200 mm.

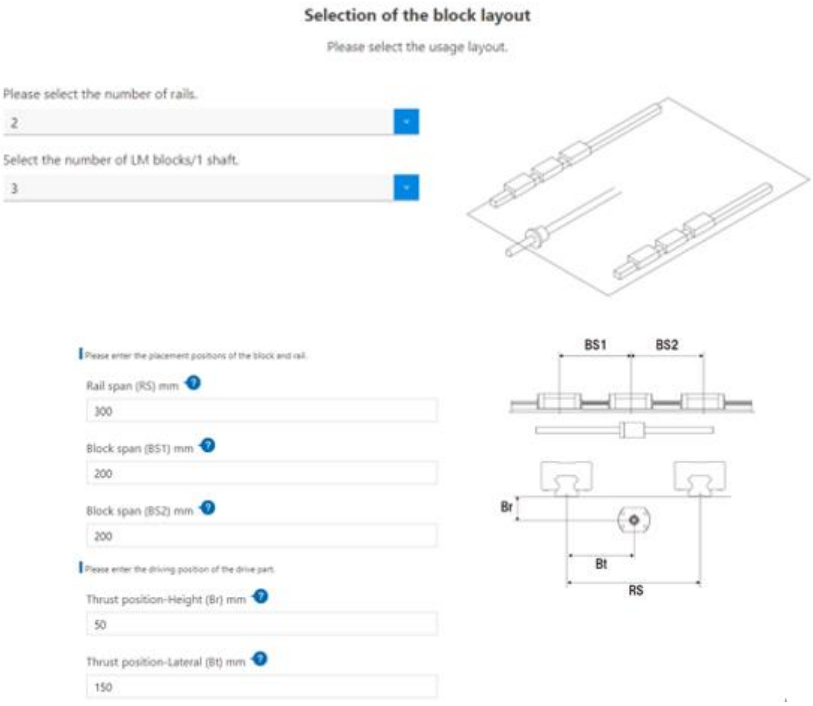

Figure 24. Software interfaces and parameters.

When the system rotates, the whole structure can be assumed to be a cantilever beam structure with two supports in 2D view as shown in Figure 25.

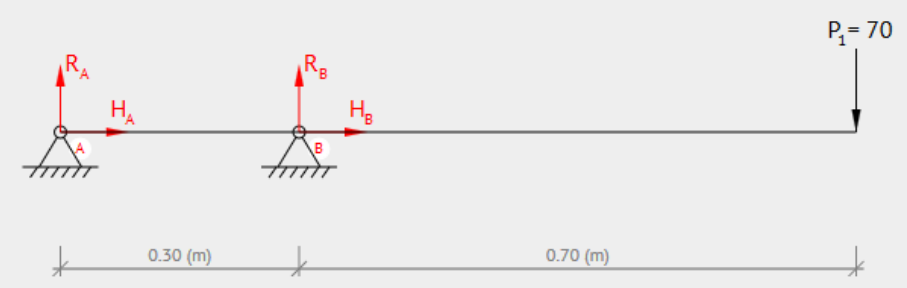

Figure 25. Freebody diagram of concept #4 after 90° rotation.

Next step is to choose the speed conditions, the cassette assembly is not like factory assembly line, the priority is to keep structure stable and move smoothly, so very low speed (250 mm/s) and low acceleration (2 m/s^2) is chosen, the stroke for each movement is around 1000 mm depends on different concepts, load coefficient is 1.2 due to the low acceleration. Frequency of use is not sure currently, but different numbers are put in the software, however, the selection result does not change. In the listed products from Table 3, number in the first column is safety factors and HSR65 series are the most desired products type.

Table 3. Listed rail guide product.

HSR65A	1.6	141	7070	Select
HSR65B	1.6	141	7070	Select
HSR65R	1.6	141	7070	Select

As mentioned in the beginning of this section. HR type rail guide is desired type, because it is mostly used in transportation application, whereas HSR type rail guide is mostly used in NC machines. However, the software does not allow change of rail guide types, instead, dimensions, load capacities and moments capacities of the selected product can be guided in choosing right HR type rail guide. There is slight difference in HSR65 series, the dimension is around 90(M)*170(W)*240(L), where M is height, W is width and L is length and its geometry illustration can be seen in Figure 26. (LM Guide, 2017, p.A1-184-185).

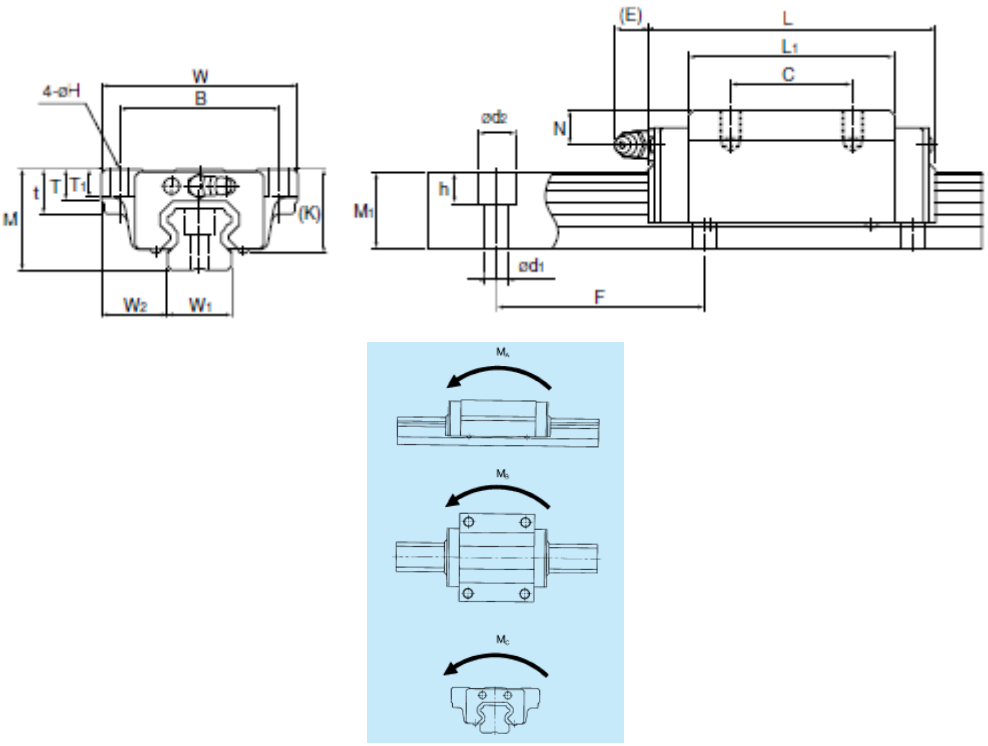

Figure 26. Geometry of chosen rail guide. (LM Guide, 2017, p.A1-184-185).

Table 4 shows the dynamic load, static load and static permissible moment in different directions from HR model, static permissible moment means static permissible moment value with one set of model HR, which includes two rails and two blocks. In another word, one set of model HR can be assumed to be one fixed support in Figure 27, the moments that blocks stand is 70 kNm. From Table 5, HR 60125 static permissible moment is 79.6 kNm when 2 blocks in close contact, which is around 10 kNm higher than calculated results and satisfy the requirements, however, after considering safer and higher stiffness, 3 sets of blocks are selected.

Table 4. Parameters of HSR 65L rail guides (LM Guide, 2017, p.A1-184-185).

	C	C_0	M_A (double block)	M_B (double block)	M_C (single block)
HSR 65L	192 kN	286 kN	35.8 kNm	35.8 kNm	8.9 kNm

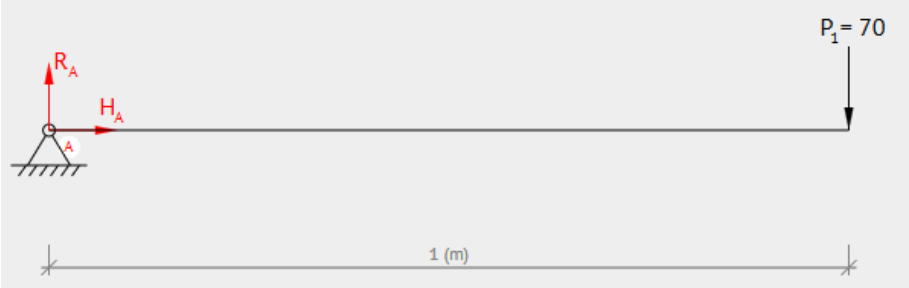

Figure 27. Freebody diagram of concept #4 in original position.

Table 5. Table of HR type rail guide parameters. (LM Guide, 2017, p.A1-264-265).

Model No.	External dimensions				LM block dimensions									
	Height M	Width W	W_R	Length L	B_1	C	H	S	h_R	L_1	T	K	Greasing hole d	D_1
HR 3065 HR 3065T	30	40.3	65	145 173.5	19	50 80	8.6	M10	9	90 118.5	27.5	29	4	14
HR 3575 HR 3575T	35	44.9	75	154.8 182.5	21.5	60 92.5	10.5	M12	12	103.8 131.5	32	34	4	18
HR 4085 HR 4085T	40	50.4	85	177.8 215.9	24	70 110	12.5	M14	13	120.8 158.9	36	38	4	20
HR 50105 HR 50105T	50	63.4	105	227 274.5	30	85 130	14.5	M16	15.5	150 197.5	45	48	5	23
HR 60125	60	74.4	125	329	35	160	18	M20	18	236	55	58	5	26

Unit: mm

	LM rail dimensions						Basic load rating		Static permissible moment kN-m*				Mass	
	Width W_1	W_R	A	Height M_R	Pitch F	d×D×h	C kN	C_0 kN	M_A 1 block	M_A 2 blocks in close contact	M_B 1 block	M_B 2 blocks in close contact	LM block kg	LM rail kg/m
	25	12	31.5	22.5	80	9X14X12	24.2 32.1	38.6 51.6	1.11 1.89	6.72 10.4	1.11 1.89	6.72 10.4	0.7 0.9	4.6
	30.5	14.5	37	26	105	11X17.5X14	30 40.2	47.8 63.6	1.53 2.59	8.84 13.5	1.53 2.59	8.84 13.5	1.05 1.4	6.4
	35	16	42.5	29	120	14X20X17	44.1 59.5	68.6 91.7	2.64 4.48	14.4 23	2.64 4.48	14.4 23	1.53 1.7	8
	42	20	51.5	37	150	18X26X22	70.7 96	107 143	5.15 8.74	28.9 45.7	5.15 8.74	28.9 45.7	3.06 3.5	12.1
	51	25	65	45	180	22X32X25	141	206	14.3	79.6	14.3	79.6	7.5	19.3

In this section, rail guide type is chosen, based on the coding example in Figure 28, the model number coding is 3 HR60125 UU +2500L UP, where 3 means three sets of LM blocks, HR60125 means the type of LM model, UU means dust prevention with end seal, +2500L means the length of the LM rail and UP means ultra-super precision grade. (LM Guide, 2017, p.A1-264).

■ **Example of model number coding**

2 HR4085T UU +1500L P

1 2 3 4 5

1 No. of LM blocks used on the same rail 2 Model number 3 Dust prevention accessory symbol (see page 17) 4 LM rail length (in mm)
5 Accuracy symbol (see page 6)

Figure 28. Coding example of rail guides. (LM Guide, 2017, p.A1-264).

The selected rail model can be seen in Figure 29 and it includes one set of rails, which is consist of two rails and two blocks.

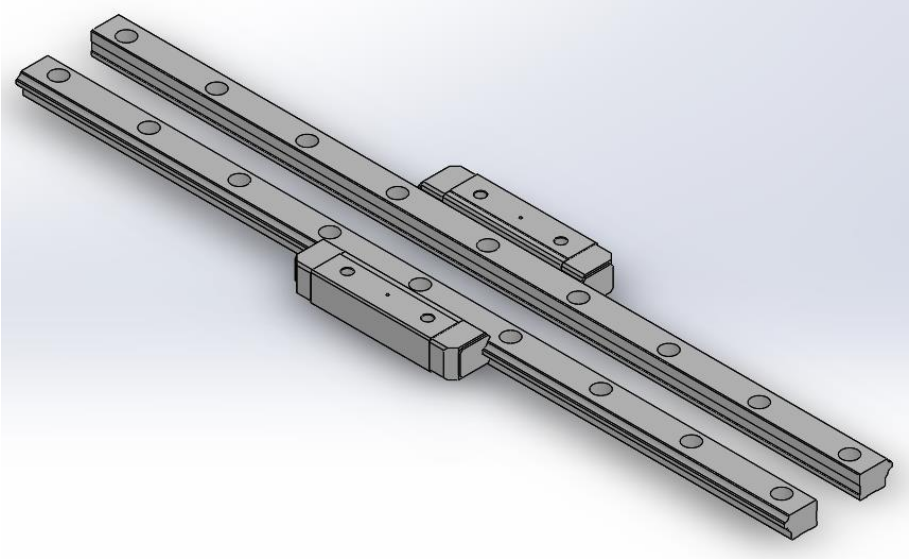

Figure 29. HR60125 guide rail model.

Spherical roller bearings

Two types of bearings are selected in the structure design. First type of bearing locates on the left side in figure, it enables the cassette to rotate around its rotating axis. This type of bearing needs to support the cassette gravity as axial load and radial load when the cassette tilt in small angle as the gravity center is not in the center of the top plate. As a result, slewing bearing is the choice in this case due to its high axial load and radial load capacities.

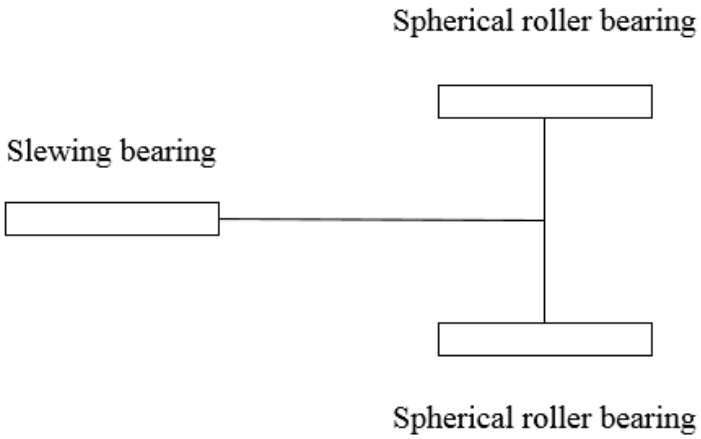

Figure 30. Bearings' locations.

Two other bearings are the same type and they are located on the right side in Figure 30, they allow the beam structure to rotate around their axis. From Table 6 below provided by NSK, here is the general bearing type selection procedure. Firstly, Self-aligning capability

is required. So, there are four bearings types, which are self-aligning ball bearings, spherical roller bearings, thrust ball bearing with aligning seat and spherical thrust roller bearings. Then bearings with higher radial loads capacity are preferred due to the high moment on the parallel manipulator side, so self-aligning ball bearings and spherical roller bearings are selected. Finally, spherical roller bearing is chosen due to the higher axial loads and it is also widely used in lots of application due to its self-aligning capability (Cao and Xiao, 2008).

Table 6. Guidelines of choosing suitable bearings (NSK 2015, p.A14-15).

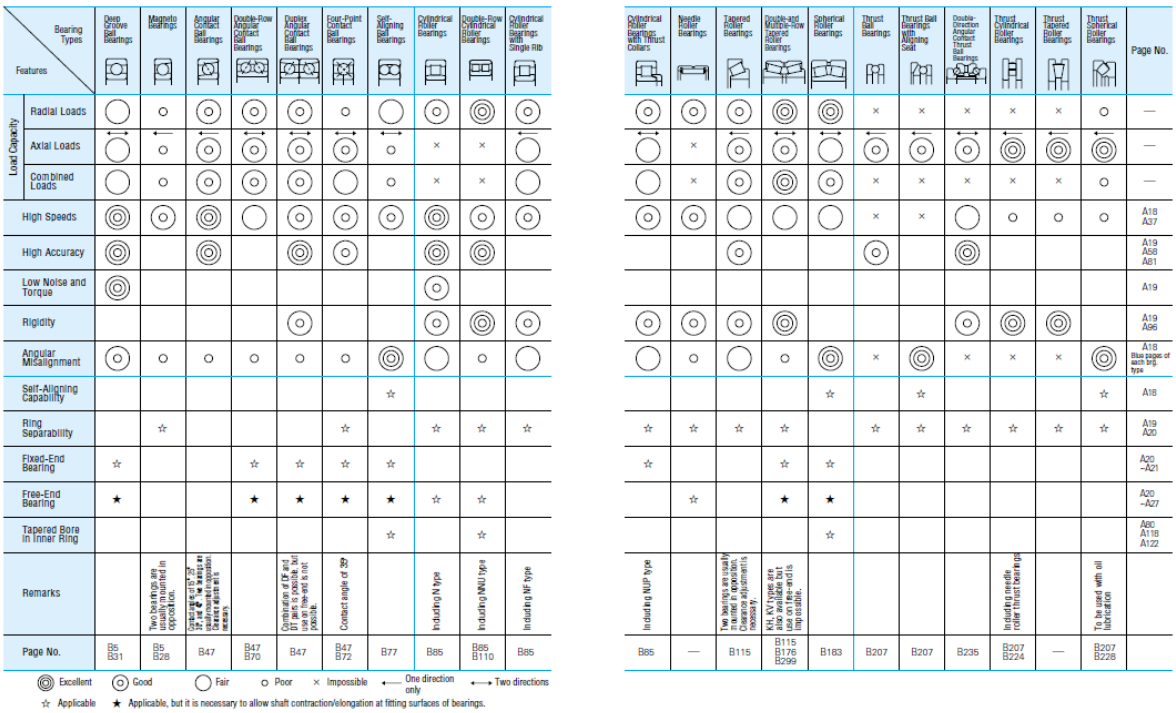

$$\left.\begin{aligned} F_r &= f_w \cdot F_{rc} \\ F_a &= f_w \cdot F_{ac} \end{aligned}\right\} \quad \cdots\cdots\cdots\cdots\cdots\cdots\cdots\cdots\cdots\cdots (5.8)$$

where F_r, F_a : Loads applied on bearing (N), {kgf}

F_{rc}, F_{ac} : Theoretically calculated load (N), {kgf}

f_w : Load factor

The values given in Table 5.5 are usually used for the load factor f_w.

Operating Conditions	Typical Applications	f_w
Smooth operation free from shocks	Electric motors, Machine tools, Air conditioners	1 to 1.2
Normal operation	Air blowers, Compressors, Elevators, Cranes, Paper making machines	1.2 to 1.5
Operation accompanied by shock and vibration	Construction equipment, Crushers, Vibrating screens, Rolling mills	1.5 to 3

Figure 31. Related formulas and factors in calculation (NSK 2005, p.A28).

The force and moment applied on spherical roller bearings can be seen in Figure 32. The gravity force of one cassette 70000 N, the distance of the beam is 1000 mm and the distance between two spherical roller bearings are 300 mm.

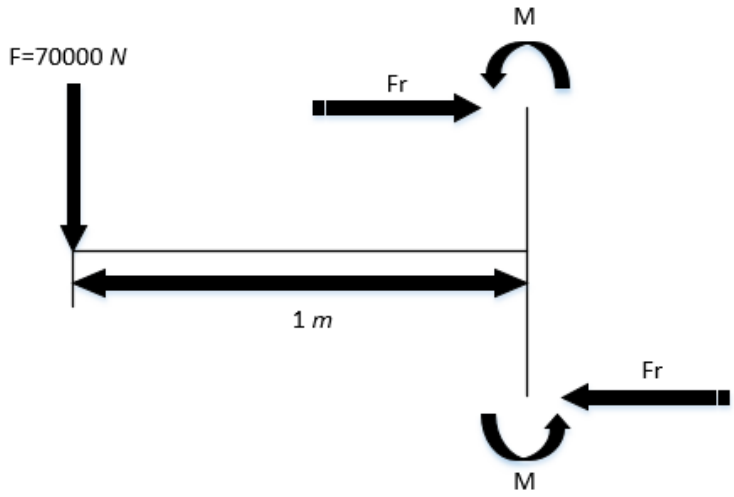

Figure 32. Freebody diagram of bearings.

After basic mathematics calculation, F_{rc}=230 kN, F_{ac}=70 kN, f_w is assumed to be 1.6 as earthquake load factor. So, F_r=372 kN, F_a=112 kN. By using the formula given in Figure 33, C_r=C_{r0}=1184 kN, from Table 7, *22324EAE4 is chosen, its geometry is illustrated in Figure 33 and its dimension can be found in Table 7. 120(d)*260(D)*86(B). And the selected spherical roller bearing 3D model can be seen in Figure 34.

Dynamic Equivalent Load

$P = XF_r + YF_a$

$F_a/F_r \leq e$		$F_a/F_r > e$	
X	Y	X	Y
1	Y_3	0.67	Y_2

Static Equivalent Load

$P_0 = F_r + Y_0 F_a$

The values of e, Y_2, Y_3, and Y_0 are given in the table below.

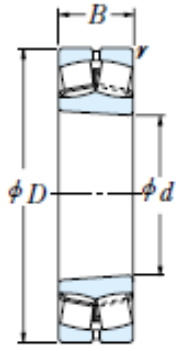

Figure 33. Formulation of bearing load calculation. (NSK 2015, p.B185).

Table 7. Bearing parameters. (NSK 2015, p.B190-191).

Boundary Dimensions (mm)				Basic Load Ratings (N)		Basic Load Ratings {kgf}		Limiting Speeds (min⁻¹)		Bearing
d	D	B	r min.	C_r	C_{0r}	C_r	C_{0r}	Grease	Oil	Cylindrical Bore
120	180	46	2	315 000	525 000	32 000	53 500	1 800	2 200	**23024CDE4**
	180	60	2	395 000	705 000	40 500	72 000	1 500	2 000	**24024CE4**
	200	62	2	465 000	720 000	47 500	73 500	1 400	1 800	**23124CE4**
	200	80	2	575 000	950 000	58 500	96 500	1 400	1 800	**24124CE4**
	215	58	2.1	685 000	765 000	70 000	78 000	2 400	3 000	***22224EAE4**
	215	76	2.1	630 000	970 000	64 500	99 000	1 300	1 700	**23224CE4**
	260	86	3	1190 000	1 320 000	122 000	134 000	1 700	2 200	***22324EAE4**

Numbers	Abutment and Fillet Dimensions (mm)					Constant	Axial Load Factors			Mass (kg)
Tapered Bore(1)	d_a min.	d_a max.	D_a max.	D_a min.	r_a max.	e	Y_2	Y_3	Y_0	approx.
23024CDKE4	130	134	170	163	2	0.22	4.5	3.0	2.9	4.11
24024CK30E4	130	131	170	158	2	0.32	3.2	2.1	2.1	5.33
23124CKE4	130	138	190	175	2	0.29	3.5	2.4	2.3	7.85
24124CK30E4	130	136	190	171	2	0.37	2.7	1.8	1.8	10
***22224EAKE4**	132	142	203	190	2	0.25	3.9	2.7	2.6	8.8
23224CKE4	132	140	203	182	2	0.34	2.9	2.0	1.9	12.1
***22324EAKE4**	134	157	246	222	2.5	0.32	3.1	2.1	2.0	22.2

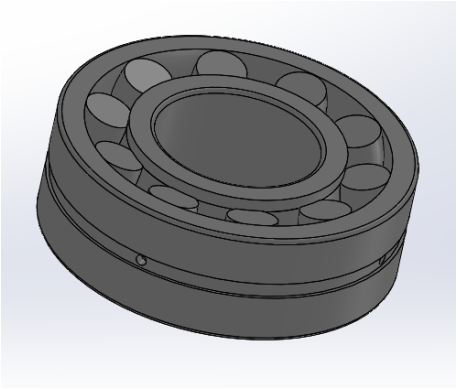

Figure 34. Spherical roller bearing*22324EAE4.

Slewing bearing

Bearing in this position stands high axial and radial forces, slewing bearing and spherical thrust roller bearings can both be chosen, but the structure of slewing bearing will give more stiffness. Moreover, slewing bearing can be integrated with outer gear so that it mates with gear and motor, this type of bearings can be used in various applications, from wind power generators to tower cranes. (Ignacio Amasorrain, 2003.)

There are three main constraints, which are geometry, force capacity and moment capacity. Firstly, the geometry need to allow the movement of structure in the chamber without collision, top plate centerline is assumed to be coincident with gravity center of cassette in top view. Secondly, the slewing bearing will hold the cassette force, safety factor is also

considered. Finally, the moment should be calculated when there is tilt angle in clearance elimination operation and the drift of gravity center point of cassette will cause moment. After all, the dynamic load is taken into consideration too since it forms when there is acceleration of structure movement. However, the acceleration needs to be controlled as small as possible during the whole operation.

In slewing bearing selection, two parameters are calculated, which are moment and force. Force is assumed to be cassette weight 70 kN. And moment is calculated when the manipulator tilt in 5°, the distance form rotation center to the mass center of cassette is assumed to be 500 mm, then calculated moment is around 3 kNm, load factor 1.5 from SKF catalog is used based on the application given in Figure 35. From SKF Kaydon bearing product catalog, MTE-210X model is chosen, whose chart can be seen in Figure 35. And the 3D CAD model can be seen in Figure 36.

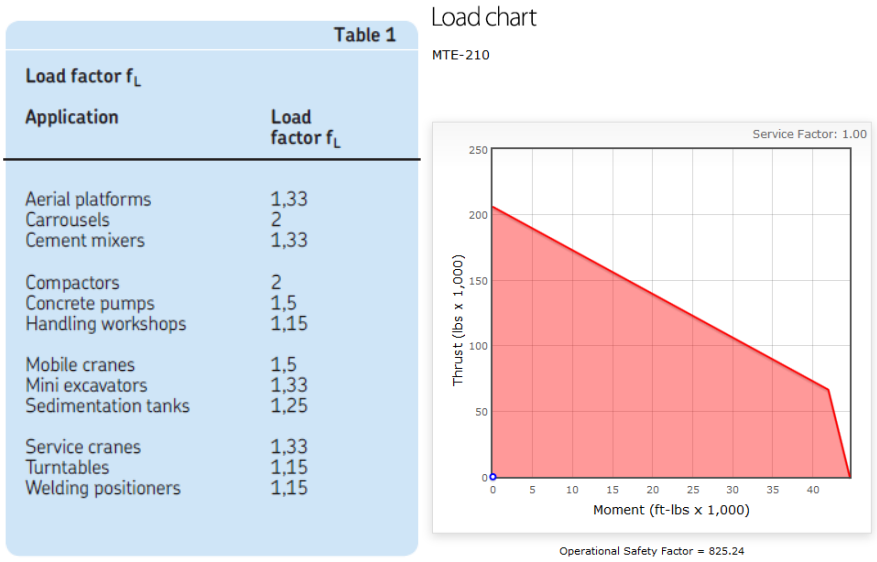

Table 1

Load factor f_L

Application	Load factor f_L
Aerial platforms	1,33
Carrousels	2
Cement mixers	1,33
Compactors	2
Concrete pumps	1,5
Handling workshops	1,15
Mobile cranes	1,5
Mini excavators	1,33
Sedimentation tanks	1,25
Service cranes	1,33
Turntables	1,15
Welding positioners	1,15

Figure 35. Slewing bearing MET-210X parameters and safety factor. (Kaydonbearings, 2017)

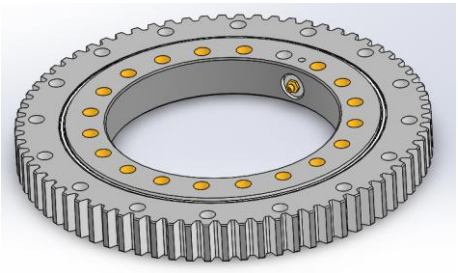

Figure 36. MET-210X model.

4-UPU parallel robot

Parallel robot can be used as robot manipulators and machine tools. Usually parallel robot is compared with serial robot. The main differences are listed below:

- Parallel manipulator has higher payload-mass ratio.
- Parallel manipulator has higher accuracy and stiffness.
- Parallel manipulator has relatively small workspace.

There are many applications built by using parallel manipulator, such as RH, machine tools, humanoid robots and medical robots. (Wu, 2008)

4-UPU parallel manipulator is parallel manipulator in universal joints-prismatic joint-universal joints structure, which can be seen in Figure 37.

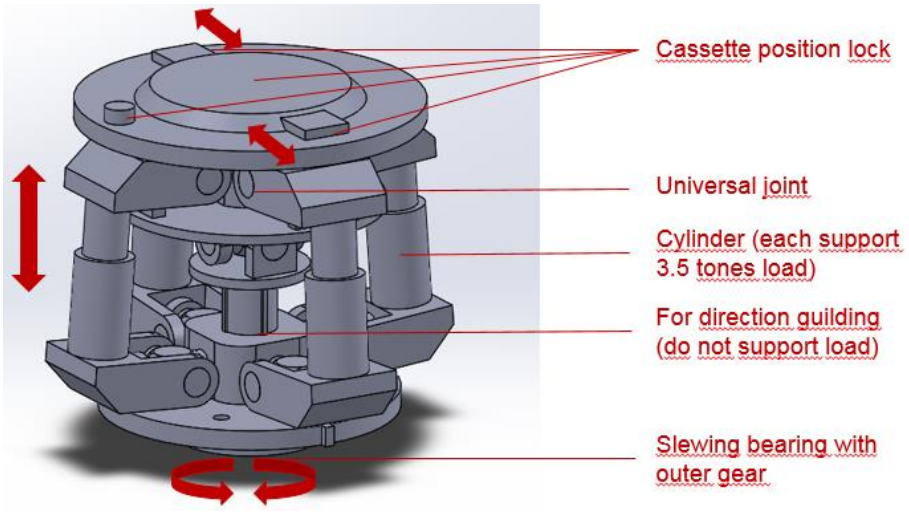

Figure 37. 4-UPU parallel manipulator structure and mechanism.

The purpose of this manipulator is to do micro adjustment after the cassette is transported to specified location, in another word, to eliminate the clearance. During the toroidal transportation of the cassette inside the vessel, there will be at least 20 mm clearance between the cassette and inner and outer blankets. An illustration of clearance locations can be seen in Figure 38.

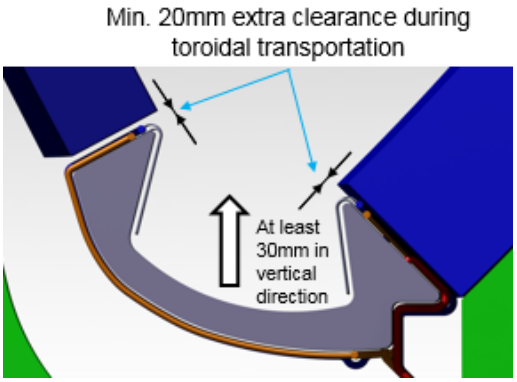

Figure 38. Clearance location of cassette during the movement (Videnoja et al., 2017).

There are four universal joints on the top side, which connect top plate and pistons, and four universal joints connect bottom plate and cylinders. In addition, there is one universal joint connect top plate and middle cylinder, which allows two directions rotation of the whole manipulator All cylinders on sides are water hydraulic actuated but cylinder in the middle is driven by other four hydraulic cylinders, the purpose of this cylinder is for controlling direction since it cannot rotate in z axis. The bottom plate is connected to slewing bearing, which can stand high load and moment at the same time.

There are three components on the top plate and they can lock the cassette, the frustum and cylinder components are fixed, they can lock the rotation movement in 3 directions, translation movements in 2 directions, the cuboid components are able to move from inside the frustum to outside and lock the cassette's translation movement in z axis. All in all, the 4-UPU parallel manipulate can rotate around x and y axis, move along z axis. Detailed parameters of cylinder extend length will be discussed in Kinematics of 4-UPU parallel manipulator.

During the lifting and descending processes in micro adjustment of 4-UPU manipulator, the whole cassette weight is applied to the four water hydraulic cylinders, the weight of one cassette is 7 tones, and each cylinder must be able to lift 3.5 tons, which is assumed to be half of the weight of the cassette. There is clearance during the toroidal transportation of the cassette inside the VV and it can be at least 20 mm clearance between the cassette and inner and outer blankets, which is illustrated in figure above.

To eliminate the clearance, the cassette should be able to move upwards 30mm, in this case, the stroke is designed to be 50 mm. From VTT water hydraulic cylinders design, cylinder's dimension is calculated by using estimated safety factor, the type of cylinder is single-acting and spring return type, the cylinder diameter is 65 mm, piston diameter is 57.2 mm, stroke length is 50 mm, retracted length is 165 mm, max pressure during the normal operation is 105 bar and max pressure during the earthquake load case is 168 bars, factor of safety during the earthquake load case (buckling) is 420.

However, in renovation concepts design, the design is focused on the reliability of cylinder, instead of using spring return, double acting cylinder is considered. Due to the space limitation, the extended height of cylinder is better to be designed around 250 mm.

In the 4-UPU manipulator, there are 4 universal joints connect piston and top plate and 4 universal joints connect cylinder and bottom plate, which allow the whole manipulator to rotate around x and y axis. In designing of universal joint phase, stress concentration is one of the most critical reason. Consider manufacturability, curvature fillet shape is usually used in cross shaft root design. The universal joints are designed based on equivalent stresses and total deformation by using ANSYS. It needs to stand heavy load especially in the concave position in universal joints, the shape of universal joint is illustrated in Figure 39.

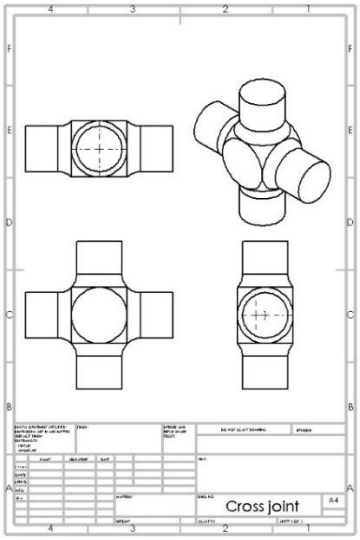

Figure 39. Universal joints drawings.

The forks are firstly welded or jointed with cylinders, pistons, top plate and bottom plates, then in assembly phase universal joints integrate them together.

In kinematics analysis of 4-UPU parallel manipulator, inverse kinematics is used (wang et al., 2009). Input data are geometry position of end-effector, which is the middle point of top plate. Coordinate systems are established based on Denavit-Hartenberg convention. The output data is extended lengths of each cylinders and tilt angle between original and final cylinders. The calculation is carried out by using Mathcad software, whose script can be seen in Figure 40.

$$\boldsymbol{R} = \begin{bmatrix} c\alpha c\beta & c\alpha s\beta s\gamma - s\alpha c\gamma & c\alpha s\beta c\gamma + s\alpha s\gamma \\ s\alpha c\beta & s\alpha s\beta s\gamma + c\alpha c\gamma & s\alpha s\beta c\gamma - c\alpha s\gamma \\ -s\beta & c\beta s\gamma & c\beta c\gamma \end{bmatrix} \quad (1)$$

$$\boldsymbol{P} = \begin{bmatrix} x \\ y \\ z \end{bmatrix} \quad (2)$$

$$\boldsymbol{d_i} = \boldsymbol{P} + \boldsymbol{R} \cdot \boldsymbol{b_i} - \boldsymbol{a_i} \quad (3)$$

$$d_i = \sqrt{[\boldsymbol{P} + \boldsymbol{R} \cdot \boldsymbol{b_i} - \boldsymbol{a_i}]^T [\boldsymbol{P} + \boldsymbol{R} \cdot \boldsymbol{b_i} - \boldsymbol{a_i}]} \quad (4)$$

In equation 1, α, β and γ are rotational angle of moving platform about Z, Y and X axis with respect to frame base plate, in this case, α=0 due to limitation of rotation around Z axis. $\boldsymbol{R}$ is rotational matrix. In equation 2, $\boldsymbol{P}$ is the vector from central point of base plate to central point of moving platform, in this case, the moving platform can only move in Z axis and rotate around X and Y axis, so x=y=0. In equation 3, $\boldsymbol{d_i}$ is the vector of the link or cylinder. $\boldsymbol{a_i}$ and $\boldsymbol{b_i}$ are vectors on base plate and moving platform that link the central and edge of the plate, which is illustrated in . In equation 4, d_i is the length of each link or cylinder.

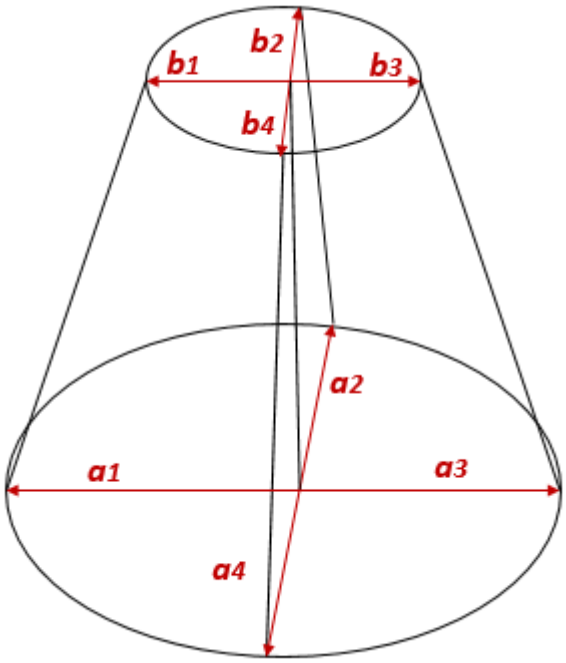

Figure 40. Kinematics analysis of 4-UPU parallel manipulator.

3.1.3 FEM analysis of concept #4

ANSYS Workbench 16.0 software is used to estimate the equivalent stresses and total deflection. Due to the limitation of nodes amounts and calculating speed consideration, some minor features and parts are suppressed during the analysis, for example, the gear and the locking system on the top plate of 4-UPU parallel manipulator. The meshing element size is 200 mm. Other parameters are default, materials chosen is stainless steel, whose parameters can be seen in Table 8. Connections in 4-UPU parallel manipulator is also built, which are eight universal joints that connect cylinders and manipulator itself.

Table 8. Parameters of stainless steel.

Properties of Outline Row 11: Stainless Steel

	A	B	C
1	Property	Value	Unit
2	Density	7750	kg m^-3
3	Isotropic Secant Coefficient of Thermal Expansion		
6	Isotropic Elasticity		
16	Tensile Yield Strength	2,07E+08	Pa
17	Compressive Yield Strength	2,07E+08	Pa
18	Tensile Ultimate Strength	5,86E+08	Pa
19	Compressive Ultimate Strength	0	Pa

As a result, the equivalent stresses and total deflection of concept #4 is calculated and can be seen in Figure 41 and Figure 42. The maximum equivalent stress is 93 MPa and total deformation is 0.15mm. These results show that the structure is safe when stainless steel is chosen since 93 MPa is smaller than its yield strength 207 MPa, and total deformation is small when it is compared to other deformation during the operation, for example, the rail might deform 1-2 cm when the temperature goes up during the operation. So, these calculating results are useful when all of 3 renovation concepts are compared, the results are not accuracy when they are compared to those existed concepts since how those models are analyzed are not clear.

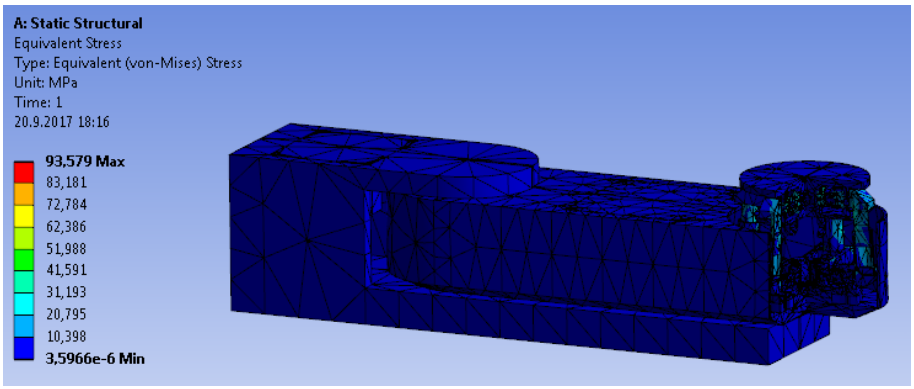

Figure 41. Equivalent stress of concept #4.

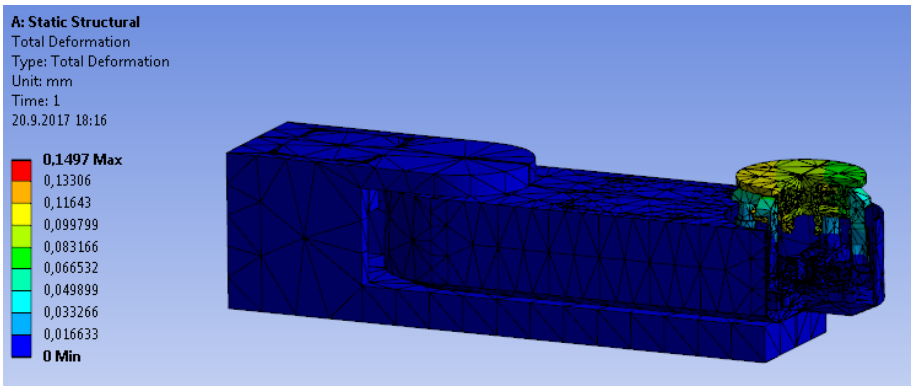

Figure 42. Total deformation of concept #4.

3.2 Concept #5

Concept #5 as shown in Figure 43 is like concept #4, the same part is the rotating beam, and the difference is in the structure mechanism or movement direction.

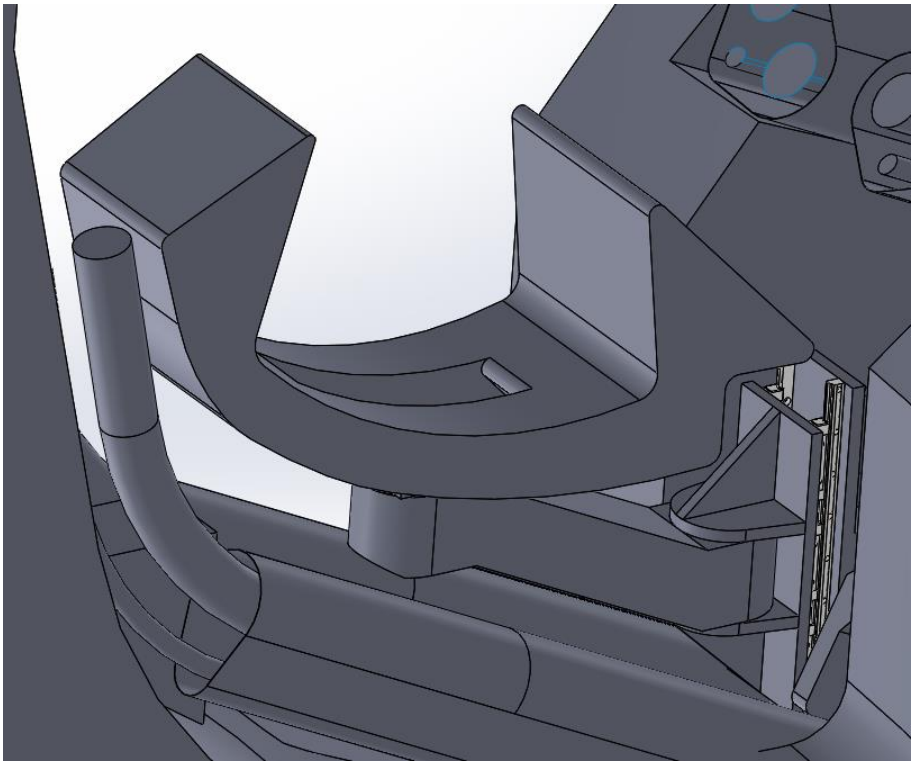

Figure 43. Concept #5 in VV.

3.2.1 Mechanism of concept #5

The concept #5 structure can be seen in Figure 44. Movement can be seen in Figure 45. Firstly, mover can provide 1st DOF, whose direction is 25° tilt from horizontal plane. Then the rail provides 2nd DOF, whose direction is up and down. These two translation joints allow the concept to move horizontally left and right in this view. There are two spherical roller bearings in vertical movement part, which is connected to the frame. These two spherical roller bearings give 3rd DOF, which allows rotation. There is one slewing bearings equipped at the bottom of the frame on the left side, which connect 4-UPU parallel manipulator and frame. With these four main components, the cassette can be moved to desired location. However, there are still some errors or clearance between desired position and real position. Therefore, micro adjustment is needed and 4-UPU parallel manipulator is required. It has 3 DOFs, which allows rotation around x and y axis and movement along z axis.

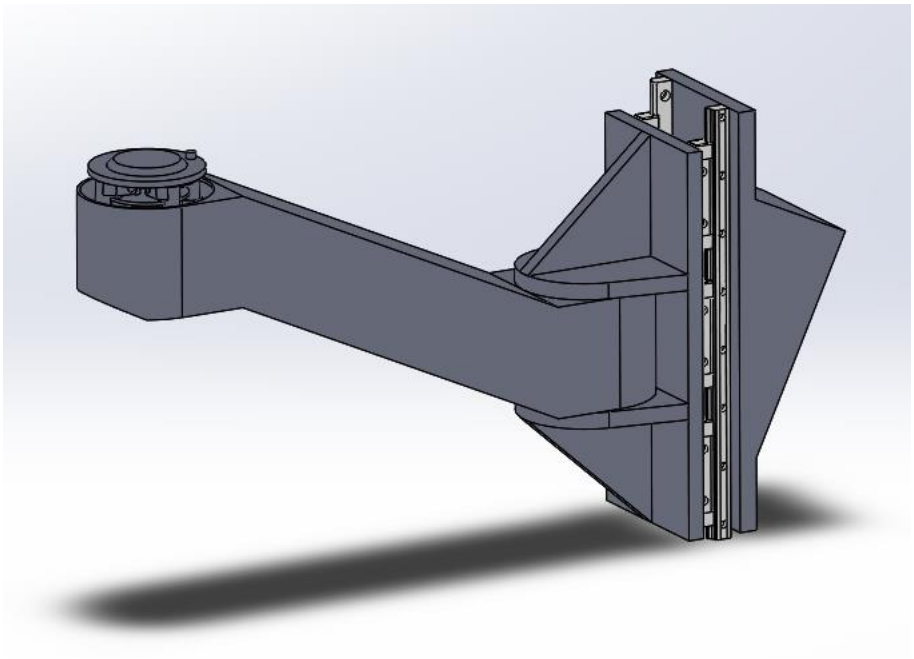

Figure 44. Overview of concept #5.

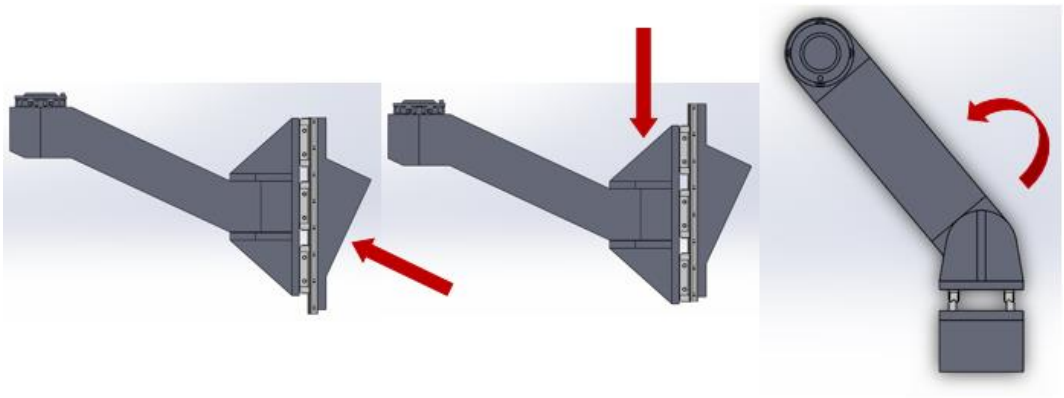

Figure 45. Concept #5 movement sequences.

3.2.2 Components of concept #5

Rail

Rail in concept #4 is horizontal, however, in concept #5, the rail is in vertical direction. So, the rail will withhold bending moment and dynamic load during the operation. The free body diagram of the whole structure can be simplified as Figure 46. The force F represent the gravity of cassette, which is 70 kN, the rail can be assumed as fixed support when the structure is in static. So, the whole structure is cantilever beam. The length of cantilever beam is 1000 mm, which is the same as concept #4, however, in this concept, there is no direct force applied vertically to the rail, there is only moment existed, which is represented

as M_A in concept #4, the moment capacity of one set of rails is 35.8 kNm, so in concept #5, 3 sets of rails are needed. The rail code is the same as concept #4, which is 3 HR60125 UU +1300L UP

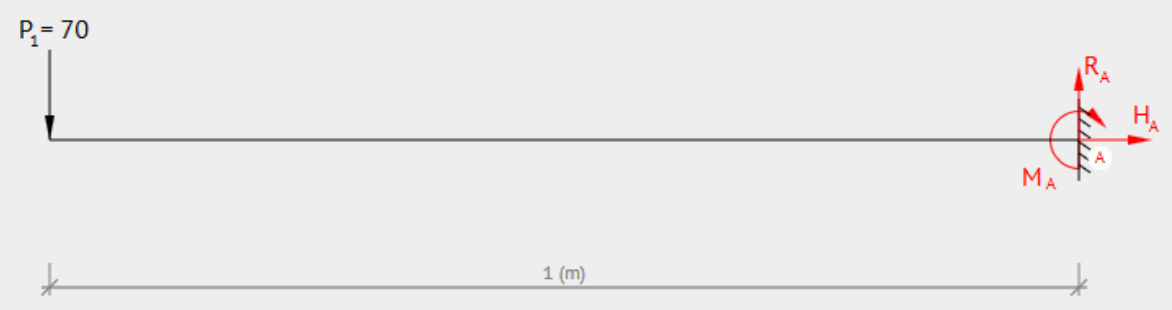

Figure 46. Free body diagram of concept #5.

Mover

Mover is the same as that in concept #4.

Spherical roller bearings

Spherical roller bearings are the same as that in concept #4, which are *22324EAE4.

Slewing bearing

Slewing bearing selection procedure is the same as that in concept #4, the chosen slewing bearing is MTE-210X.

4-UPU parallel manipulator

4-UPU parallel manipulator is the same as that in concept #4.

3.2.3 FEM analysis of concept #5

In this section, equivalent stresses and total deformation of concept #5 are analyzed. Due to the licenses limitation and to shorten the calculation time, the models are simplified without changing the main structure. The gears, rail and bearings are suppressed because they are all complicated components. The guide rail is also suppressed, and the surface connected to rail guide is set to be fixed support. In addition, the force is 70 kN and it applies on the top plate of 4-UPU manipulator, the connection between cylinder and plates are selected as universal joint connection. The analysis results of concept #5 can be seen in Figure 47 and Figure 48. The maximum equivalent stress is 84 MPa and total deformation is 1.13 mm.

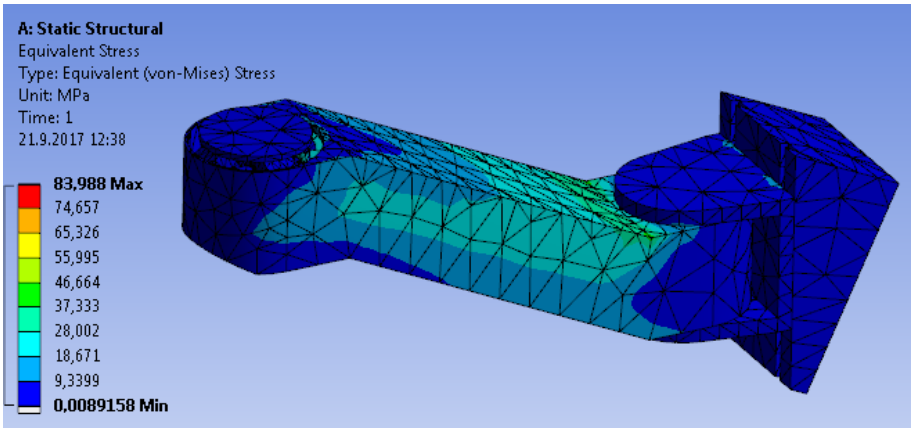

Figure 47. Equivalent stress of concept #5.

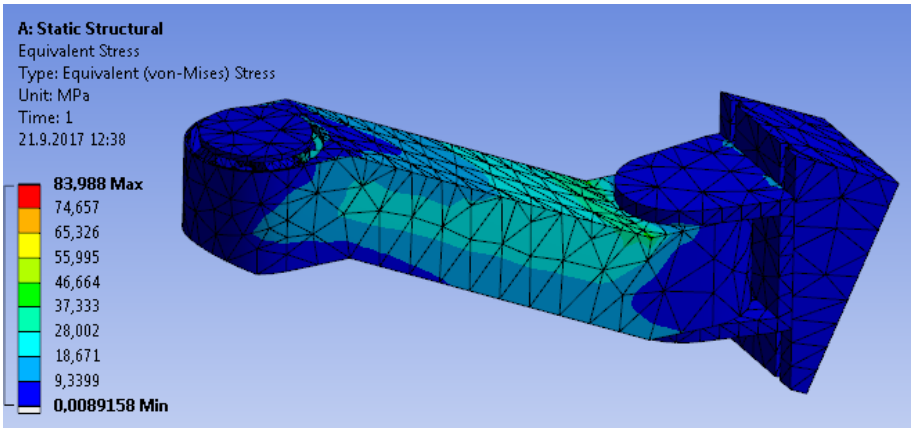

Figure 48. Total deformation of concept #5.

3.3 Concept #6

Concept #6 in VV is shown in Figure 49.

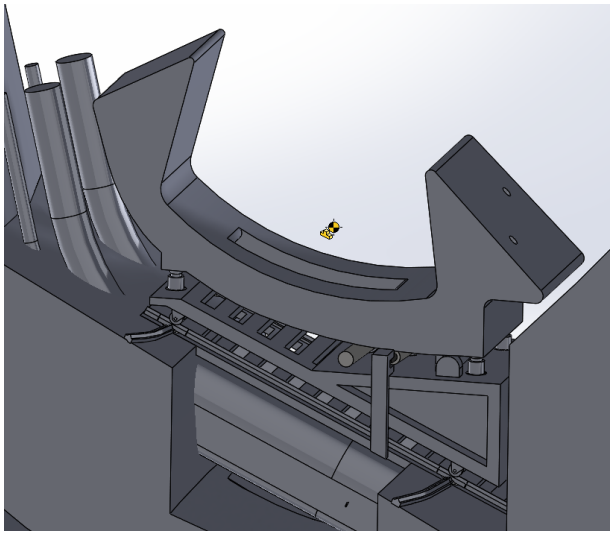

Figure 49. Concept #6 in VV.

3.3.1 Mechanism of concept #6

In concept #6, 4-UPU parallel manipulator is not in used. Instead, a simple supported beam structure is used. This structure is different from other two cantilever structures and it is simple but reduce the development costs (Mozzillo et al., 2017). The surface of VV is modified to allow the plate lay on the VV surface instead of edge, an illustration of the support or contact area can be seen in Figure 51. The plate is designed with some hollow section to reduce the weight of the whole body so that the mover can transport the plate and put it on the VV surface. Once the plate is in location, it will be locked with help of two cylinders on the two sides of the plate and one block in the front of the plate. The cylinder is buried inside the plate initial and it can move when the plate is put in position. The structure can be seen in Figure 50.

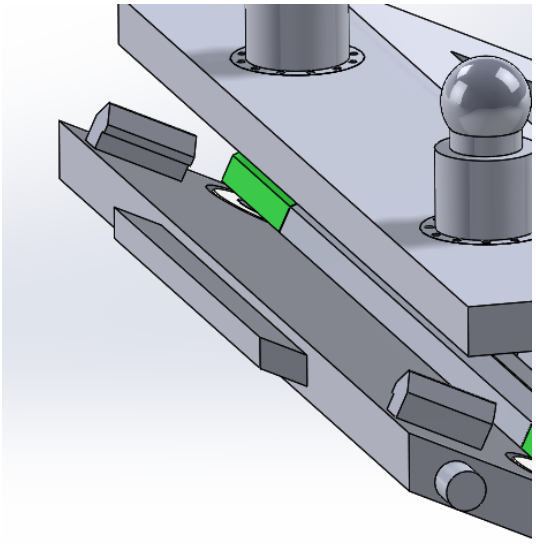

Figure 50. Lock system of the plate.

However, there are some modification on the VV surface and cassette bottom. The surface of VV is modified to allow the plate lay on the VV surface instead of edge, an illustration of the support or contact area can be seen in Figure 51. A lock bar is added at the bottom of the cassette as shown and two roller with 60 mm diameters are added vertically on the plate, so that the combination of lock bar and two rollers can limit the cassette movement along horizontal direction.

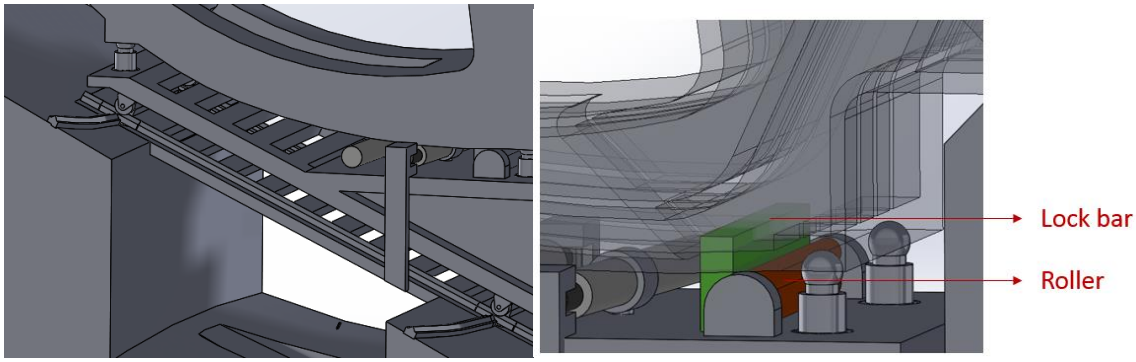

Figure 51. Contact area between plate and VV surface.

The modification of cassette bottom is illustrated in Figure 52. In VV, there should be rail installed and it can be connected to the rail on the plate. The concept #6 structure can be seen in Figure 53 and movement sequences can be seen in Figure 54. Part 1 is hydraulic jack, there are four hydraulic jacks, each of them have stoke of 50 mm, and they are connected to cassette's base as spherical joint. Part 1 and part 7 are connected by bearing housing. Part 2 is double acting, single piston, telescopic cylinder, part 3 is connection part between cylinder and part 4, and it can rotate around z axis. Part 4 and part 7 work as platforms, which allow all components to be integrated. Part 5 is rail connection system, which will be introduced in following sections. Part 6 is connected to cylinder by revolute joint and it is rigid body when integrated with part 4 during the movement, when the cylinder is not needed, it disconnects with part 4 and only connects with cylinder.

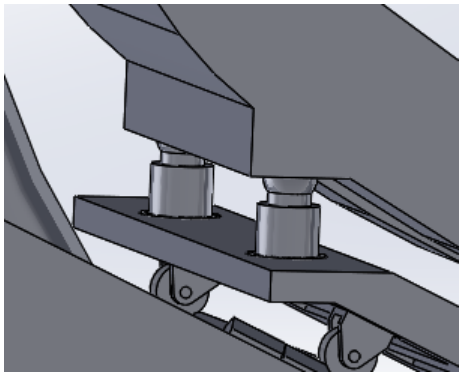

Figure 52. Modification of cassette bottom and lock system

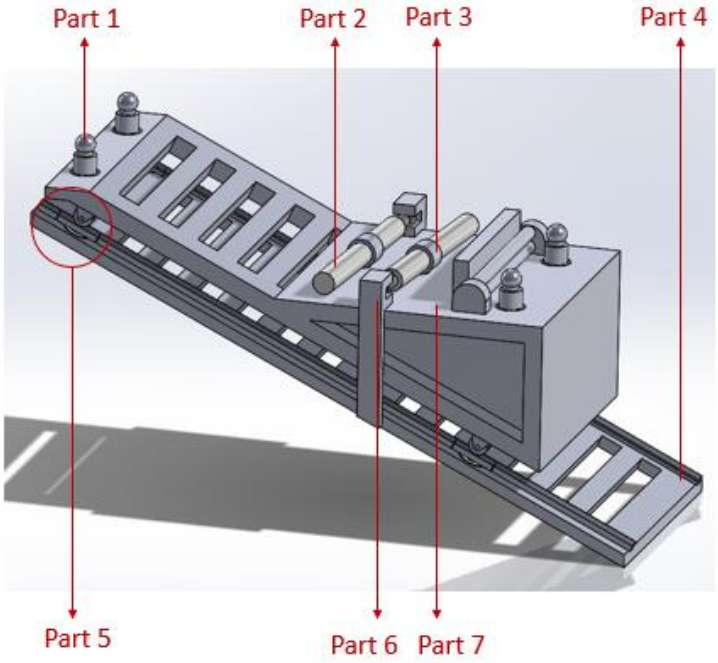

Figure 53. Concept #6 structure.

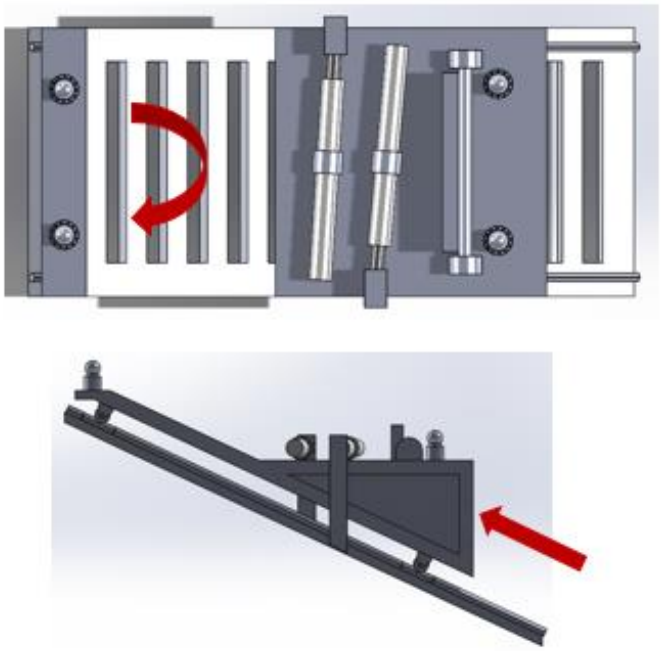

Figure 54. Concept #6 movement sequences.

About the rail connection system, it is illustrated in Figure 55. Part 8 is V-shape rail, rail 1 and rail 2 are the same type. Part 9 is V-shape bearing on the rail. Part 10 is spherical roller bearing, it connects part 9 and part 7. Part 11 is spherical roller bearing, it connects part 8

and part 4. Rail 1 is straight rail on the part 4. Rail 2 is rail on the part 4. When cassette is transported along y axis to desired location, rail connection system will rotate 90°, part 8 will connect with rail 1 to integrate toroidal rail on the VV surface and allow cassette movement along toroidal direction. The end of every rail related to rotation should be curved to avoid collision.

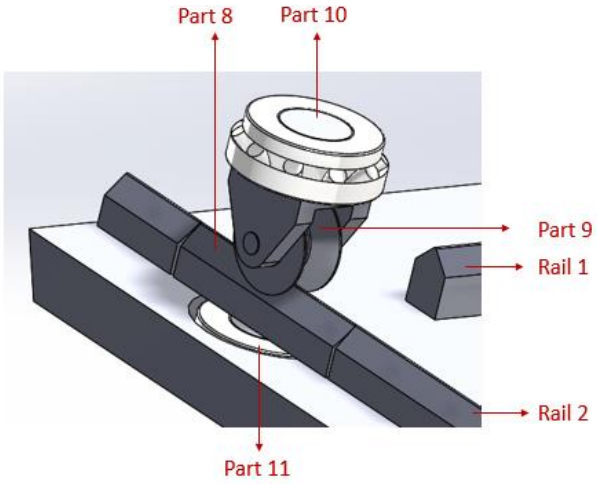

Figure 55. Rail change system.

And the rail structure before and after rail change can be seen in Figure 56 and Figure 57 separately.

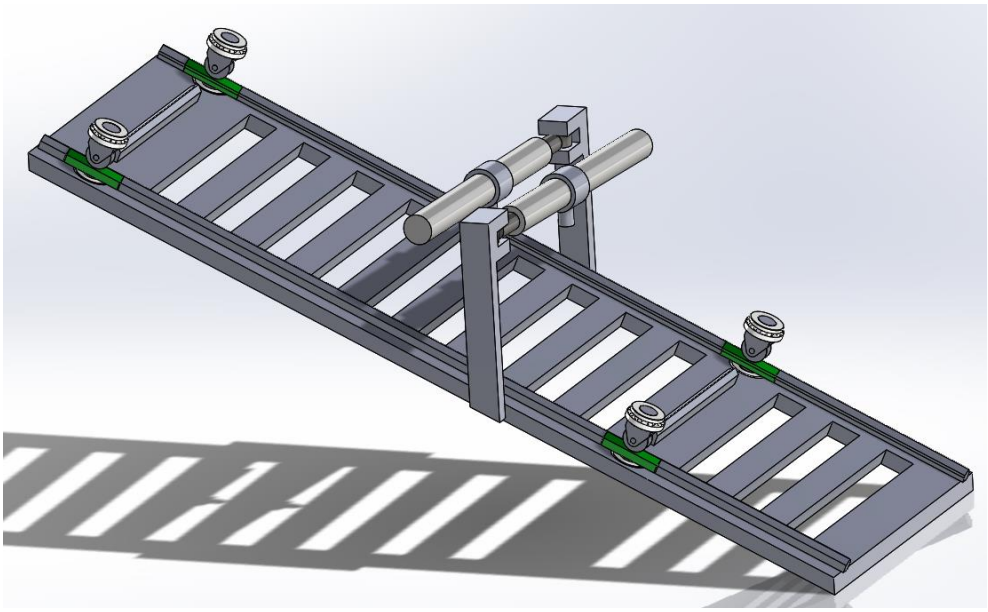

Figure 56. Rail before change.

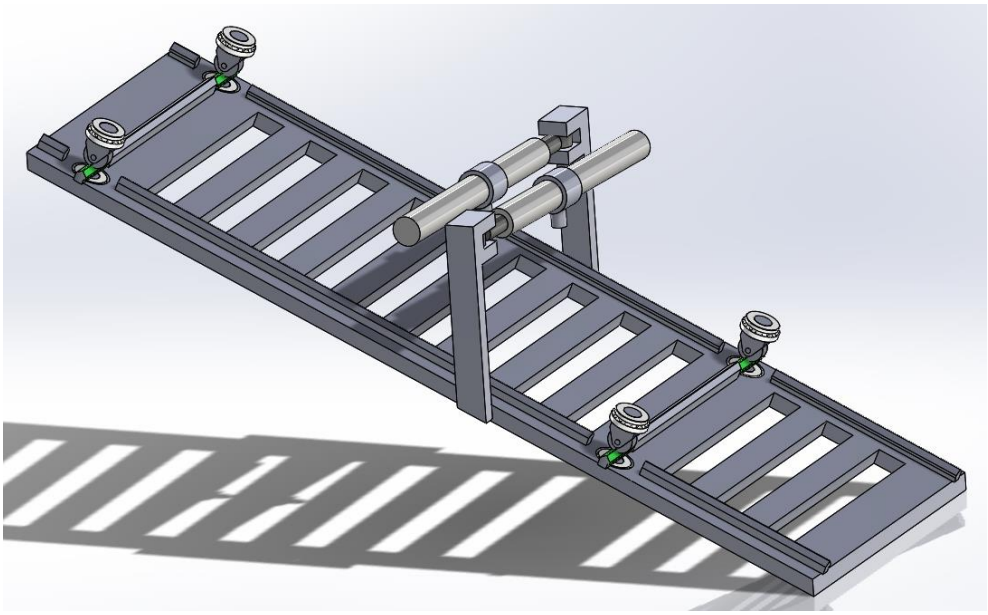

Figure 57. Rail after change.

About the movement mechanism of the structure. Firstly, mover provide 1st DOF, which transport the whole system in 25° angle tilted from horizontal plane. 2nd DOF is provide by cylinders, there are two cylinders equipped, and each cylinder will control the movement in one direction. Bearings and rails will rotate 90° to form toroidal rail so that when cylinder pushes the cassette and connected plate, the structure can follow the rail to desired location. About micro adjustment, there are four hydraulic jacks on the 4 corners of the plate connected to cassette. It can lift and descend to eliminate the clearance and mate two cassettes together.

3.3.2 Components of concept #6

Rail

Different from previous two concepts, rail in concept #6 has a 25° incline angle from horizontal surface. V shape rails and V shape bearings are used in this concept since they allow movement along both straight and curve rail. Each V shape bearing should be able to hold half weight of the cassette (Videnoja et al., 2017). So that each V shape bearings should have 3.5 tones capacity, after taking 25° incline angle into consideration, the V shape bearings should have 3.1 tones capacity in radial direction. As a result, the selected bearing is MVYR-62 tapered roller bearing, which can be seen in Figure 58. As for the rail, it is selected from the same company as the bearing As MSRP-1 type, which can be seen in

Figure 59. But the width can be designed to be wider than the manufacturer to avoid possible deformation during radiation, the width of the rail is designed to be 60 mm.

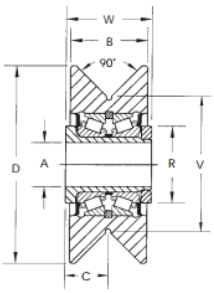

MVYR

V-Groove Yoke Style

SMITH-TRAX®

General Information

The **Smith-Trax®** Series bearings are designed and manufactured to handle increased axial and radial loads by using **Tapered Roller Bearings** or **Deep Groove Ball Bearings**. These bearings should be used when standard needle roller bearings are not sufficient to handle the thrust load found in certain applications. Consult our Engineering Department for special requirements.

Dimensional Data (mm)

SMITH Bearing® Number	BEARING TYPE TRB-Tapered Roller Bearing	D Roller O.D.	B Groove Dia.	A Bore Diameter +0.00 -0.02	W Overall Width	V Point Diameter	C Groove Center	R Shoulder or End Plate Diameter 33 rpm.	Radial Basic Dynamic Rating (N) 500 hrs. 33 rpm.	Dynamic Thrust Load Rating (N) 500 hrs.
MVYR-62	TRB	90	38	20	40	62	22	32.0	48,400	17,800
MVYR-76	TRB	110	44	25	46	76	23	44.5	63,600	25,700
MVYR-100	TRB	140	54	30	56	100	28	57.2	78,200	25,600
MVYR-125	TRB	165	68	45	71	125	36	82.6	148,100	58,500
MVYR-150	TRB	190	70	55	73	150	37	88.9	159,200	63,000
MVYR-200	TRB	240	76	70	79	200	40	108.0	188,600	77,400
MVYR-250	TRB	290	76	70	79	250	40	108.0	188,600	77,400

Figure 58. V-Groove Yoke Style (Smith bearing product catalog, 2017).

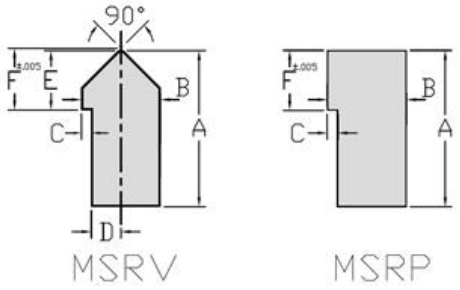

Compare Products

	Name	(A)	(B)	(E)	(F)	(C)	
☐	MSRP-1XXXX	75 mm	40 mm	27 mm	28.2 mm	6 mm	Add to Quote
☐	MSRP-2XXXX	100 mm	50 mm	39 mm	40.6 mm	6 mm	Add to Quote
☐	MSRV-1XXXX	75 mm	40 mm	27 mm	28.2 mm	6 mm	Add to Quote
☐	MSRV-2XXXX	100 mm	50 mm	39 mm	40.6 mm	6 mm	Add to Quote

Figure 59. V-shape rail (Smithbearing.com, 2017).

Cylinders

Cylinders are needed to actuate the movement along the toroidal rail, the friction coefficient is around 0.05, the mass of cassette is 70000 kg, then the force needed from cylinder is 3500 kN, then robot arm is not considered, for example, SCARA robot maximum load is 100-150 kg. As a result, hydraulic cylinder is selected. The cylinder maximum length can be the same as the width of part 2, which is 1200 mm, the stroke length is found out by geometry of two adjacent cassettes, which is 900 mm. Two hydraulic cylinders are selected and each one control one direction movement. About connection part of cylinder, the details can be seen in Figure 60. Take right side cylinder as example, the bottom plate is connected to piston by revolute joint, when there is stroke, the reactionary force will push the cassette and top platform do toroidal movement along the rail on the VV.

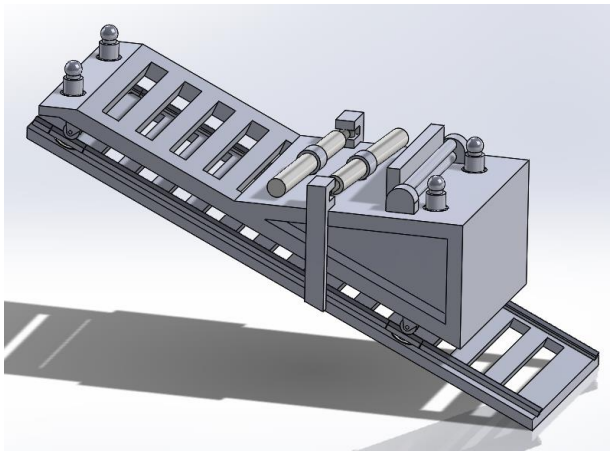

Figure 60. Concept #6 structure.

Due to the geometry limitation, the stroke is almost the same length as cylinder, so telescopic cylinder is chosen as in the Figure 61, here is one telescopic cylinder parameters of one manufacturer. It is double acting telescopic cylinder and actuates the movement along toroidal rail, each cylinder actuate movement in one direction, and stroke is around 2-3 times longer than cylinder's original length. The length of cylinder is limited to 800 mm based on model geometry, the stroke length should be more than 900 mm based on the model geometry. There is also limitation of cylinder's diameter due to the distance between the structure and cassette bottom surface, which should be below 200 mm, as a result, cylinder diameter is 150 mm, cylinder length is 800mm, stroke length is 900 mm, there are 4 extension stages in stroke, max working pressure is 160 bars.

IM-T64 modenflex Interpump Hydraulics International

CILINDRO TELESCOPICO DOPPIO EFFETTO
DOUBLE ACTING TELESCOPIC CYLINDER
DOPPELWIRKENDER TELESKOPZYLINDER

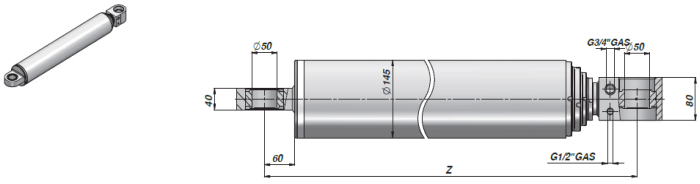

Codice Code Bestell-Nr.	Serie	Sfilate Extensions Stufenzahl	Corsa Stroke Hub	Pressione massima di lavoro Max Working Pressure Maximumbetriebsdruck bar	Z	kg
IMT641600800	T64/160	4	1850	160	800	59
IMT641601000	T64/160	4	2650	160	1000	74
IMT641601100	T64/160	4	3050	160	1100	81
IMT641601200	T64/160	4	3450	160	1200	88

Figure 61. Telescopic cylinder parameters (IM-T64 telescopic cylinders, 2017).

Spherical roller bearings

There are 8 spherical roller bearings, which connect to block and cassette connection plate on one side, connect rail and bottom plate on another side. The cassette weight 7 tons, it is assumed that 4 tones mass is applied on each bearing in vertical direction. Due to the structure requirement, the bearings are assembled in 25° angle tilted from horizontal plane, therefore, the free body diagram can be seen in Figure 62.

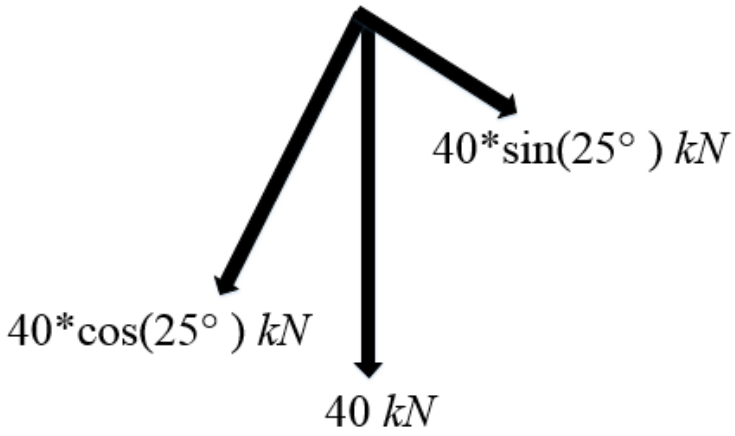

Figure 62. Freebody diagram of force applied on bearing.

F_r is calculated as 17 kN and F_a is calculated as 36 kN, safety factor is chosen from Figure 31 given in previous section, which is 1.5. Then by using the formula given in the NSK rolling bearings book, which is shown in Figure 33. The calculated results are C_a=338 kN, C_{0a}=502 kN, From given Table 9, the selected spherical thrust roller bearing is 29413E, whose d=65 mm, D=140 mm and T=45 mm and 3D model is illustrated in Figure 63.

Table 9. Spherical roller bearing parameters (NSK 2015, p.B186-187).

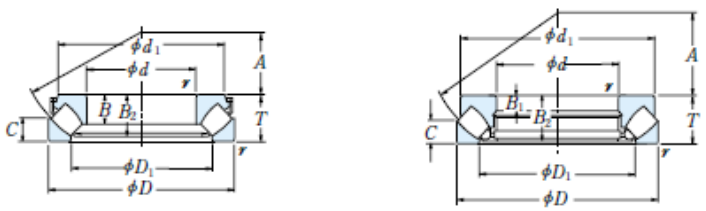

Boundary Dimensions (mm)				Basic Load Ratings (N)		Basic Load Ratings (kgf)		Limiting Speeds (min⁻¹) Oil	Bearing Numbers
d	D	T	r min.	C_a	C_{0a}	C_a	C_{0a}		
60	130	42	1.5	330 000	885 000	33 500	90 000	2 600	**29412 E**
65	140	45	2	405 000	1 100 000	41 500	112 000	2 400	**29413 E**

Table 10 continues. Spherical roller bearing parameters (NSK 2015, p.B186-187).

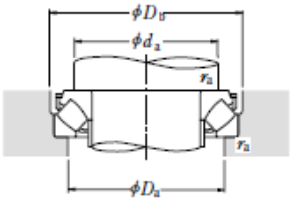

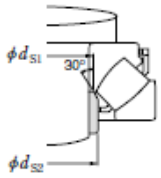

Dynamic Equivalent Load

$P = 1.2F_r + F_a$

Static Equivalent Load

$P_0 = 2.8F_r + F_a$

However, $F_r/F_a \leq 0.55$ must be satisfied.

Dimensions (mm)						Spacer Sleeve Dimensions (mm)		Abutment and Fillet Dimensions (mm)				Mass (kg)
d_1	D_1	B, B_1	B_2	C	A	d_{S1} max.	d_{S2} max.	d_a(1) min.	D_a max.	D_b min.	r_a max.	approx.
114.5	89	27	38	20	38	67	67	90	108	133	1.5	2.55
121.5	93	29.5	40.5	22	42	72	72	100	115	143	2	3.2

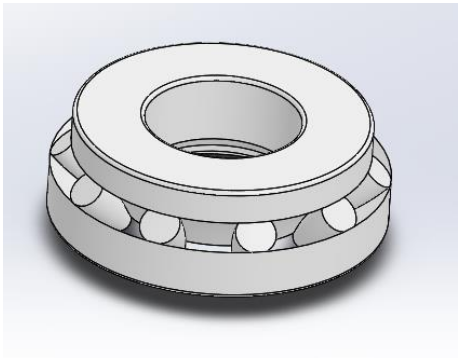

Figure 63. Spherical roller bearing model

Hydraulic jack

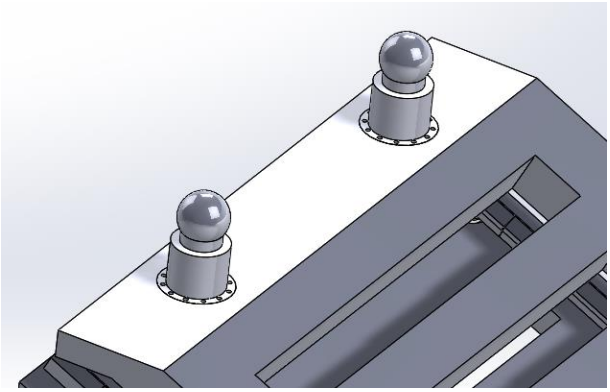

Figure 64. Hydraulic jack model.

There are four hydraulic jacks on part 7, the tips of hydraulic jack are manufactured to ball shape and connected to the bottom surface of cassette as spherical joints. The reason of

designing this ball shape is to allow the cassette rotation movement around x and y axis. Furthermore, it allows micro movement on z axis about 50 mm, which is meant for eliminating the clearance between cassette inner and outer blanket.

There are limited space between cassette bottom surface and part 7 top surface, which is shown in Figure 65 and it is around 100-200 mm depends on different locations. The diameter of cylinder is 60 mm, each cylinder can hold 3.5 tones, which is half weight of the cassette.

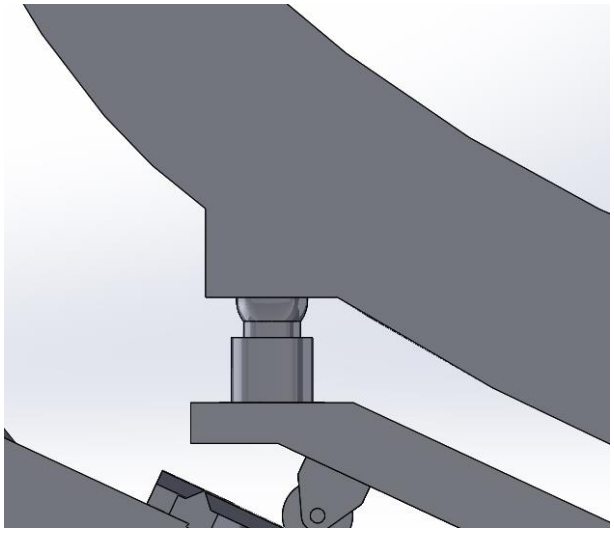

Figure 65. Space between concept #6 and cassette.

In the market, there is single acting, spring return cylinders, whose chart can be seen in Table 11. The smallest cylinder capacity in this manufacturer is 5 tones, which is higher than needed capacity. The selected cylinder mode number is RC-53 the collapsed is 165 mm and stroke is 76 mm, which satisfies the space requirement of concept #6.

Table 11. Single acting, spring return cylinders. (Enerpac.com, 2017)

Cylinder Capacity	Stroke	Model Number	Cylinder Effective Area	Oil Capacity	Collapsed Height	Weight
ton (kN)	mm		cm^2	cm^3	mm	kg
5 (45)	16	RC-50**	6,5	10	41	1
	25	RC-51	6,5	16	110	1
	76	RC-53	6,5	50	165	1,5
	127	RC-55*	6,5	83	215	1,9
	177	RC-57	6,5	115	273	2,4
	232	RC-59	6,5	151	323	2,8

However, once the spring in cylinder loses its effectiveness, the cylinder is invalid. So double acting cylinder is more reliable. From the same manufacturer, the double acting cylinder can be seen in Table 12. The lowest cylinder capacity is 10 tones, which is much higher than needed cylinder capacity as well as the stroke. As a result, the cylinder needed to be designed. The suggested double acting cylinder parameters are:

- Cylinder capacity: 3.5 tones
- Stroke: 50 mm
- Collapsed length: 200 mm
- Outside diameters: 60 mm

Table 12. Double acting cylinder (Enerpac.com, 2017).

Cyl. Capacity	Stroke	Model Number	Max. Cylinder Capacity		Effective Area		Oil Capa-city		Coll. Height	Ext. Height	Out-side Dia.	Wt.
			kN		cm^2		cm^3					
ton (kN)	mm		Push	Pull	Push	Pull	Push	Pull	mm	mm	mm	kg
10	254	**RR-1010**	101	33	14,5	4,8	368	122	409	663	73	12
(101)	305	**RR-1012**	101	33	14,5	4,8	442	147	457	762	73	14

3.3.3 FEM analysis of concept #6

In this section, equivalent stresses and total deformation of concepts #3 are analyzed. Due to the licenses limitation and to shorten the calculation time, the models are simplified without changing the main structure. Some components such as spherical roller bearings and rail guide are suppressed because they are all complicated components that can make the structure mesh complicated. Since the bearings and rail guide dimension are calculated to be able to undertake the load so these components analysis do not contribute the analysis. The bottom of the plate is assumed to be fixed support and forces are applied vertically to the cylinders. In addition, the force is 70 kN and equivalent stress and total deformation can be seen in Figure 66 and Figure 67. The maximum equivalent stress is 2.4931 MPa and total deformation is 0.0024 mm.

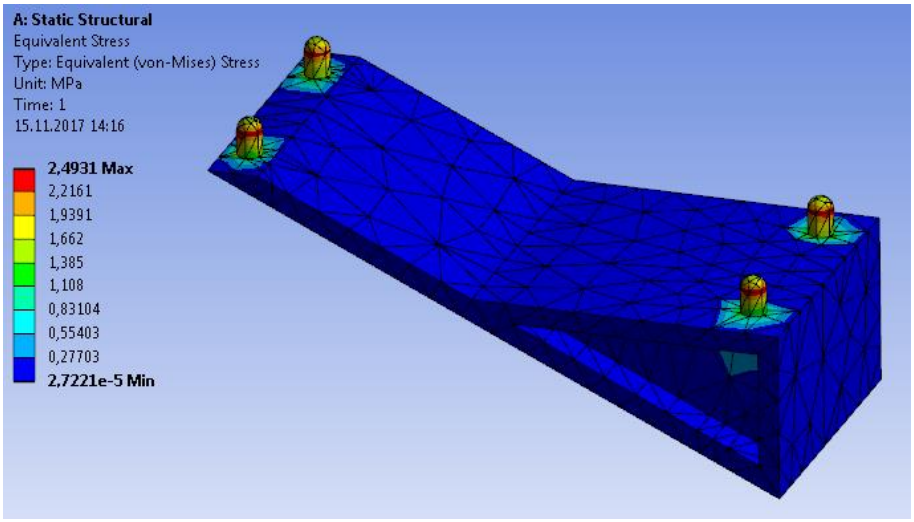

Figure 66. Equivalent stress of concept #6.

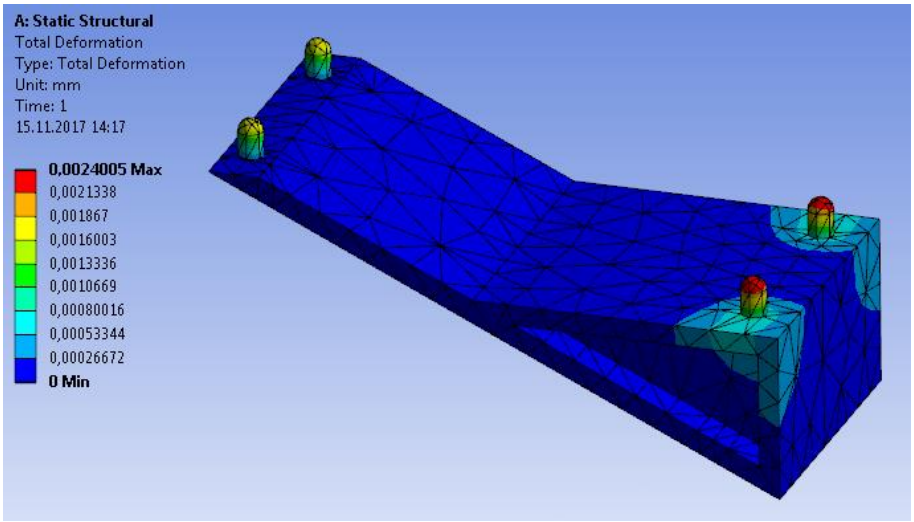

Figure 67. Total deformation of concept #6.

3.4 Future work of innovational concepts

Overall structures of cassette RH end-effector are carried out and here are future works that should be considered:

- Detailed FEM analysis: due to the license limitation and computing speed reduction, each concept is simplified and analyzed, for example, bearings and rails are suppressed because these components will generate large amount of mesh in calculation.
- Interfaces and sensors: Interfaces and sensors will be considered to provide vision and accuracy operation.

- Detailed actuator components design: Some actuator components are not selected but only space of actuator is reserved, such as motor.
- Reliability design: reliability design will be carried out, the backup plan when there is breakdown in the end-effector happens should be carried out.

4 SIX CONCEPTS ANALYSIS

In this chapter, all the concepts are compared, the advantages and disadvantages of each concepts are listed. However, the comparison based on the function between 3 innovational concepts and 3 existed concepts is more reliable than FEM results since the preset parameters of existed concepts are unknown. But the FEM analysis results can be used to check which concept is relatively better in stiffness.

4.1 Three innovational concepts comparison

3 concepts are shown in Figure 68 and comparison are listed below.

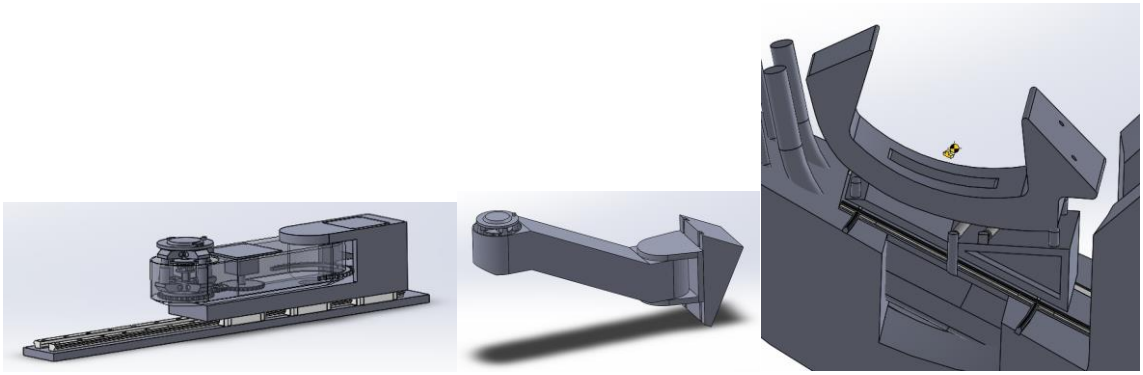

Figure 68. Concept #4, #5 and #6.

In concept #4, here lists some comparison between other concepts:

- Rail is connected both to cassette and mover so that concept #4 gives greater stiffness than concept #5
- Movement is independent of mover once the rail is in position
- Mover can remove the whole structure out once there is break down in structure due to some mechanical reasons, such as cylinder leakage and motor break down.

In concept #5, here lists some comparison between other concepts:

- Mover is one part of the manipulator; its movement integrated with vertical movement has the same effect of horizontal movement as that in concept #4.
- It is cantilever structure and it has longer beam than concept #4, so the structure has more deformation than concept #4.

- It can move up and down, so there is more space, which allow longer cylinders, space movement flexibility and more space for components, such as motor.

In concept #6, here lists some comparison between other concepts:

- The mass center of cassette is in an area, which is surrounded by four hydraulic jacks. As a result, it gives more stiffness to the whole structure even if there is dynamic shock or tilt angle compared to other concepts.
- It needs rail installed beforehand in VV, which might cause some accuracy problems since there can be 1 cm to 2 cm deformation in rail when the system is in the operation.
- There is no cantilever structure in this concept so that this concept has smaller deformation on sides. In reliability concern, if some break or emergency maintenance are needed inside the structure such as cylinder leakage, motor breakdown. The whole structure can be pulled out by string simply by following the rail. Since the structure locates on the rail, it will not fall, which might be problem in other 2 concepts.

About FEM analysis results. The reliability of the results can only be applied on the comparison among these three innovative concepts. Because simplified models are used due to license limitation. Another reason is that the parameters such as model, force, support location and environment of FEM analysis from existed concepts are unknown. However, other parameters such as forced applied on the model, support location, connection between each components are carefully chosen to keep consistency. Environment such as radiation and temperature are not taken into consideration since the radiation may result unexpected deformation. The results can be used to compare the stiffness of these three concepts.

The equivalent stress and total deformation of concept #6 are much lower than those of concept #4 and concept #5, which mean concept #6 has greater stiffness. The reason is concept #6 use more simple structure without too many links, which is used in concept #4 and concept #5 as 4-UPU parallel manipulator, there can be some huge equivalent stress and deformation happens in the links of 4-UPU parallel manipulator.

4.2 Three existed concepts comparison

Three concepts are shown in Figure 69 and comparison are listed below.

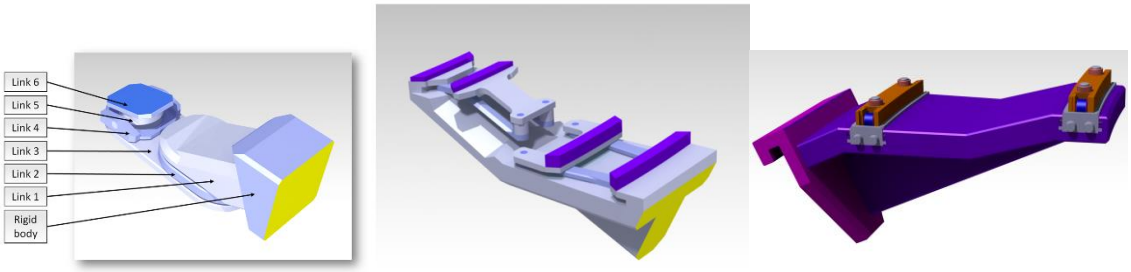

Figure 69. Concept #1, #2 and #3 (Videnoja et al., 2017).

In concept #1, here lists some comparison between other concepts:

- It has good flexibility since the manipulator can eliminate alignment errors and displacements of the frame.
- There is no toroidal rail in the VV and interfaces for the end-effector are not needed inside the VV.
- Since it is cantilever structure so that the weight of the cassette is totally supported by mover and by the cantilever beam.
- There is limited space for the cassette interfaces because joints 4, 5 and 6 have the same space as cassette interface.

In concept #2, here lists some comparison between other concepts:

- It has good load capacity since the cassette is supported around its gravity center and it is supported on both sides.
- It might be good for rescue if there is some broken inside the structure.
- Space is required inside the vessel for load supporting interfaces.
- Here are still conflict with the blanket pipes.

In concept #3, here lists some comparison between other concepts:

- There is less deflection compared to other two concepts due to the non-cantilevered structure.
- It allows good access to space allocated for the cassette outboard fixation.
- It is low profile solution for toroidal transportation of the adjacent cassettes.

- It is asymmetrical design, there is space between the inboard and outboard hydraulic jacks and they perform the toroidal transportation of the cassette by moving the hydraulic jacks.
- There are permanent rails prone to neutron damage, hydraulic jacks can get stuck due to the tritium dust and other particles.
- Design is currently asymmetrical, so that left and right cassette require mirrored end-effectors.
- After fixation, cassette deflection could cause unwanted loads to the lifting cylinders.

After all these comparison, here are mainly two different types of structures, which are cantilever and simply supported beams. Moreover, each of them has its own merits.

Table 13 illustrates the key aspects among six concepts, which include structure type, the dependence of mover on cassette transports process, the utilization of 4 UPU parallel manipulator and the modification on VV surface.

Table 13. Key aspects among six concepts

	Structure	Mover	4 UPU parallel manipulator	Modification on VV surface
Concept #1	Cantilever	Independent	No	No
Concept #2	Simple two sides supported	Independent	No	Rail installation
Concept #3	Simple two sides supported	Independent	No	Rai installation
Concept #4	Cantilever	Dependent	Yes	Light
Concept #5	Cantilever	Dependent	Yes	No
Concept #6	Simple two sides supported	Independent	No	Rail installation

5 CONCLUSION

In this thesis, three innovational concepts of divertor RH end-effector are introduced, the mechanism of the manipulator is the most crucial part in this thesis, especially in limited space. What comes next is the components selection of each components, concept #4 and concept #5 have some components in common, such as 4-UPU parallel manipulator. However, in concept #6, the structure is quite different from others, some structures need to be designed in totally new way, such as rail system. Some improvements can be noticed from these innovative concepts, such as utilization of mover system and rail structure. There are also some components that all concepts have but different in dimension, such as bearings, in bearings selection, bearing is selected by its load capacity and function. SOLIDWORKS 2017 software and ANSYS Workbench 16.0 software are used in this conceptual design.

Furthermore, comparison of three innovational concepts and existed concepts are carried out. Merits and demerits of each concept are analyzed when they are compared to each other.

In the following work, efforts will be focused on other detailed components selection, such as motor and gear selection. Also, reliability of the end-effector concepts will be the main part in following work. Design in this thesis does not consider radiation, if radiation is taken into consideration, there will be much difference, because the radiation will cause unexpected deformation on the structure and the structure might be locked and become rigid. As a result, the measures or operations once the end-effector fails should be carried out.

LIST OF REFERENCES

Aymar, R. (1997). ITER overview. Fusion Engineering and Design, 36(1), pp.9-21.

Bak, J., Yang, H., Oh, Y., Park, Y., Park, K., Choi, C., Kim, W., Sa, J., Kim, H. and Lee, G. (2006). Status of the KSTAR tokamak construction. Fusion Engineering and Design, 81(20-22), pp.2315-2324.

Cao, M. and Xiao, J. (2008). A comprehensive dynamic model of double-row spherical roller bearing—Model development and case studies on surface defects, preloads, and radial clearance. Mechanical Systems and Signal Processing, 22(2), pp.467-489.

Carfora, D., Di Gironimo, G., Järvenpää, J., Huhtala, K., Määttä, T. and Siuko, M. (2015). Divertor remote handling for DEMO: Concept design and preliminary FMECA studies. Fusion Engineering and Design, 98-99, pp.1437-1441.

DCHAIN-SP 2001: High Energy Particle Induced Radioactivity Calculation Code. (2001). JAERI-Data/Code 2001-016.

Di Gironimo, G., Cacace, M., Crescenzi, F., Labate, C., Lanzotti, A., Lucca, F., Marzullo, D., Mozzillo, R., Pagani, I., Ramogida, G., Roccella, S. and Viganò, F. (2015). Innovative design for FAST divertor compatible with remote handling, electromagnetic and mechanical analyses. Fusion Engineering and Design, 98-99, pp.1465-1469.

Di Gironimo, G., Labate, C., Renno, F., Brolatti, G., Crescenzi, F., Crisanti, F., Lanzotti, A., Lucca, F. and Siuko, M. (2013). Concept design of divertor remote handling system for the FAST machine. Fusion Engineering and Design, 88(9-10), pp.2052-2056.

Di Pietro, E., Barabaschi, P., Kamada, Y. and Ishida, S. (2014). Overview of engineering design, manufacturing and assembly of JT-60SA machine. Fusion Engineering and Design, 89(9-10), pp.2128-2135.

Doshi, B., Zhou, C., Ioki, K., Xie, H., Gupta, G., Bhardwaj, A. and Terasawa, A. (2011). ITER Cryostat—An overview and design progress. Fusion Engineering and Design, 86(9-11), pp.1924-1927.

Enerpac.com. (2017). Single Acting Hydraulic Cylinder: RC Series | Enerpac. [online] Available at: http://www.enerpac.com/en/industrial-tools/hydraulic-cylinders-jacks-lifting-products-and-systems/general-purpose-hydraulic-cylinders/rc-series-single-acting-hydraulic-cylinders [Accessed 17 Nov. 2017].

English.ipp.cas.cn. (2017). EAST Achieves Longest Steady-state H-mode Operations---- Institute of Plasma Physics Chinese Academy Of Scieneces. [online] Available at: http://english.ipp.cas.cn/syxw/201611/t20161115_170479.html [Accessed 4 Dec. 2017].

EurekAlert!. (2017). China's 'artificial sun' sets world record with 100s steady-state high performance plasma. [online] Available at: https://www.eurekalert.org/pub_releases/2017-07/caos-cs070517.php [Accessed 4 Dec. 2017].

Federici, G., Kemp, R., Ward, D., Bachmann, C., Franke, T., Gonzalez, S., Lowry, C., Gadomska, M., Harman, J., Meszaros, B., Morlock, C., Romanelli, F. and Wenninger, R. (2014). Overview of EU DEMO design and R&D activities. Fusion Engineering and Design, 89(7-8), pp.882-889.

Gryaznevich, M. and Asunta, O. (2017). Overview and status of construction of ST40. Fusion Engineering and Design, 123, pp.177-180.

Holtkamp, N. (2007). An overview of the ITER project. Fusion Engineering and Design, 82(5-14), pp.427-434.

Ignacio Amasorrain, J. (2003). Load distribution in a four contact-point slewing bearing. Mechanism and Machine Theory, 38(6), pp.479-496.

IM-T64 telescopic cylinders. (2017). [ebook] Contarini, p.1. Available at: http://www.contarini.net/dms/Sito%20Contarini/PDF%20schede/Schede%20cat%20A%20iet/im-t64_pdf.pdf [Accessed 19 Nov. 2017].

Ioki, K. (1995). Design of the ITER vacuum vessel. Fusion Engineering and Design, 27(1-2), pp.39-51.

ITER. (2017). Fusion. [online] Available at: https://www.iter.org/sci/whatisfusion [Accessed 17 Nov. 2017].

ITER. (2017). The divertor. [online] Available at: https://www.iter.org/mach/divertor [Accessed 17 Nov. 2017].

ITER. (2017). Tokamak. [online] Available at: https://www.iter.org/mach/Tokamak [Accessed 17 Nov. 2017].

ITER. (2017). What is ITER?. [online] Available at: https://www.iter.org/proj/inafewlines [Accessed 17 Nov. 2017].

Janeschitz, G., Borrass, K., Federici, G., Igitkhanov, Y., Kukushkin, A., Pacher, H., Pacher, G. and Sugihara, M. (1995). The ITER divertor concept. Journal of Nuclear Materials, 220-222, pp.73-88.

Kaydonbearings. (2017). Load chart MET-210X. [online] Available at: https://www.kaydonbearings.com/load_chart.htm/MTE-210 [Accessed 19 Nov. 2017].

Macklin, B., Bao, L., Chappuis, P., Escourbiac, F., Gicquel, S., Palmer, J., Raffray, R., Wilson, D., Humphreys, S., Norman, M., Diez, S. and Wagrez, J. (2015). Assembly and remote handling of ITER plasma facing components. 2015 IEEE 26th Symposium on Fusion Engineering (SOFE).

Maisonnier, D. (2008). European DEMO design and maintenance strategy. Fusion Engineering and Design, 83(7-9), pp.858-864.

Maisonnier, D., Martin, E. and Palmer, J. (2001). ITER R&D: Remote Handling Systems: Divertor Remote Handling Systems. Fusion Engineering and Design, 55(2-3), pp.259-271.

McAdams, R. (2014). Beyond ITER: Neutral beams for a demonstration fusion reactor (DEMO) (invited). Review of Scientific Instruments, 85(2), pp.02B319.

MCNP – A General Monte Carlo N-Particle Transport Code, Version 5. (2003). LANL report, LA-CP-03-0245, (rev. March 2005) April.

Mitchell, N., Bauer, P., Bessette, D., Devred, A., Gallix, R., Jong, C., Knaster, J., Libeyre, P., Lim, B., Sahu, A. and Simon, F. (2009). Status of the ITER magnets. Fusion Engineering and Design, 84(2-6), pp.113-121.

Mitchell, N., Bessette, D., Gallix, R., Jong, C., Knaster, J., Libeyre, P., Sborchia, C. and Simon, F. (2008). The ITER Magnet System. IEEE Transactions on Applied Superconductivity, 18(2), pp.435-440.

Mozzillo, R., Di Gironimo, G., Mäkinen, H., Miccichè, G. and Määttä, T. (2017). Concept design of DEMO divertor cassette remote handling: Simply supported beam approach. Fusion Engineering and Design, 116, pp.66-72.

Mozzillo, R., Marzullo, D., Tarallo, A., Bachmann, C. and Di Gironimo, G. (2016). Development of a master model concept for DEMO vacuum vessel. Fusion Engineering and Design, 112, pp.497-504.

Nielsen, J. (1993). Iterative user-interface design. Computer, 26(11), pp.32-41.

NSK. 2005. [NSK webpage]. Updated 2005. [Referred 2005]. Available: http://www.jp.nsk.com/app01/en/ctrg/index.cgi?rm=pdfView&pno=e1102m.

Pacher, H. (1997). Erosion lifetime of ITER divertor plates. Journal of Nuclear Materials, 241-243(1), pp.255-259.

Palmer, J., Siuko, M., Agostini, P., Gottfried, R., Irving, M., Martin, E., Tesini, A. and Uffelen, M. (2005). Recent developments towards ITER 2001 divertor maintenance. Fusion Engineering and Design, 75-79, pp.583-587.

Raffray, A., Calcagno, B., Chappuis, P., Fu, Z., Furmanek, A., Jiming, C., Kim, D., Khomiakov, S., Labusov, A., Martin, A., Merola, M., Mitteau, R., Sadakov, S., Ulrickson, M. and Zacchia, F. (2014). The ITER blanket system design challenge. Nuclear Fusion, 54(3), p.033004.

Rolfe, A. (1999). Remote handling JET experience. JET Joint Undertaking, pp.1-5.

Smithbearing.com. (2017). Products - Manufacturer of Smith Bearing Cam Followers by Accurate Bushing. [online] Available at: http://www.smithbearing.com/Products/147/SMITH-Rail/MSRV-MSRP-Metric-Guide-Rails [Accessed 19 Nov. 2017].

Smith bearing product catalog. (2017). [ebook] Garwood: Accurate Bushing Company, p.59. Available at: http://www.rotaprecision.com/pdf/ABC-Catalog2004.pdf [Accessed 19 Nov. 2017].

Someya, Y., Utoh, H., Hiwatari, R., Tanigawa, H. and Tobita, K. (2017). Shutdown dose-rate assessment during the replacement of in-vessel components for a fusion DEMO reactor. Fusion Engineering and Design, 124, pp.615-618.

Song, Y., Wu, S., Li, J., Wan, B., Wan, Y., Fu, P., Ye, M., Zheng, J., Lu, K., Gao, X., Liu, S., Liu, X., Lei, M., Peng, X. and Chen, Y. (2014). Concept Design of CFETR Tokamak Machine. IEEE Transactions on Plasma Science, 42(3), pp.503-509.

Song, Y., Wu, S., Wan, Y., Li, J., Ye, M., Zheng, J., Cheng, Y., Zhao, W. and Wei, J. (2014). Concept design on RH maintenance of CFETR Tokamak reactor. Fusion Engineering and Design, 89(9-10), pp.2331-2335.

Thomas, J., Loving, A., Bachmann, C. and Harman, J. (2013). DEMO hot cell and ex-vessel remote handling. Fusion Engineering and Design, 88(9-10), pp.2123-2127.

Tivey, R., Ando, T., Antipenkov, A., Barabash, V., Chiocchio, S., Federici, G., Ibbott, C., Jakeman, R., Janeschitz, G., Raffray, R., Akiba, M., Mazul, I., Pacher, H., Ulrickson, M. and Vieider, G. (1999). ITER divertor, design issues and research and development. Fusion Engineering and Design, 46(2-4), pp.207-220.

Videnoja, J., Lyytinen, J., Sibois, R., Venho-Ahonen, O. and Siuko, M. (2017). Divertor Cassette Transporter & Platform Proof of Principle Design – Concept Design Review. AWP2016-RM-3.2.2-T001-D005.

Wang, Y., Pessi, P., Wu, H. and Handroos, H. (2009). Accuracy analysis of hybrid parallel robot for the assembling of ITER. Fusion Engineering and Design, 84(7-11), pp.1964-1968.

Wu, H. (2008). Parallel manipulators, towards new applications. Vienna, Austria: I-Tech.

Wu, S. (2007). An overview of the EAST project. Fusion Engineering and Design, 82(5-14), pp.463-471.

You, J., Mazzone, G., Visca, E., Bachmann, C., Autissier, E., Barrett, T., Cocilovo, V., Crescenzi, F., Domalapally, P., Dongiovanni, D., Entler, S., Federici, G., Frosi, P., Fursdon, M., Greuner, H., Hancock, D., Marzullo, D., McIntosh, S., Müller, A., Porfiri, M., Ramogida, G., Reiser, J., Richou, M., Rieth, M., Rydzy, A., Villari, R. and Widak, V. (2016). Conceptual design studies for the European DEMO divertor: Rationale and first results. Fusion Engineering and Design, 109-111, pp.1598-1603.

You, J., Visca, E., Bachmann, C., Barrett, T., Crescenzi, F., Fursdon, M., Greuner, H., Guilhem, D., Languille, P., Li, M., McIntosh, S., Müller, A., Reiser, J., Richou, M. and Rieth, M. (2016). European DEMO divertor target: Operational requirements and material-design interface. Nuclear Materials and Energy, 9, pp.171-176.

Zhao, W., Song, Y., Wu, H., Cheng, Y., Peng, X., Li, Y., Wei, J. and Mao, X. (2015). Concept design of the CFETR divertor remote handling system. Fusion Engineering and Design, 98-99, pp.1706-1709.